DEVELOPING THE POLYCYSTIC KIDNEY DISEASE INTERACTOME

By

Mackenzie Brauer

Bachelor of Science, Royal Military College of Canada, 2017

A thesis presented to Ryerson University
in partial fulfillment of the requirements for the degree of Master of Science
in the program of Molecular Science

Toronto, Ontario,
Canada, 2020

AUTHOR'S DECLARATION FOR ELECTRONIC SUBMISSION OF A THESIS

I hereby declare that I am the sole author of this thesis. This is a true copy of the thesis, including any required final revisions, as accepted by my examiners.

I authorize Ryerson University to lend this thesis to other institutions or individuals for the purpose of scholarly research.

I further authorize Ryerson University to reproduce this thesis by photocopying or by other means, in total or in part, at the request of other institutions or individuals for the purpose of scholarly research.

I understand that my thesis may be made electronically available to the public.

DEVELOPING THE POLYCYSTIC KIDNEY DISEASE INTERACTOME

Mackenzie Brauer

Master of Science

Molecular Science

Ryerson University, 2020

Abstract

Autosomal Dominant Polycystic Kidney Disease (ADPKD) is a genetic disease causing numerous renal cysts to form leading to adult renal failure. The PKD-causing genes, polycystic kidney disease-1 and -2 (PKD1 and PKD2), encode for proteins polycystin-1 and -2 (PC1 and PC2). These proteins form a complex through their C-termini at cilia with mutations abolishing their interaction and impairing ciliary localization. We report the first use of proximity-dependent biotinylation for identification (BioID) to characterize the PC1 PC2 C-terminal complex binding partners in HEK 293 cells. We identify high-confidence interacting partners including an enrichment of cilia-related, transporter activity and trafficking genes. We report interesting PC1 interactions including Biogenesis of Lysosome-Related Organelles Complex-1 (BLOC-1) subunits and BLOC-One-Related Complex (BORC) subunits. We also report endoplasmic reticulum (ER)-related proteins that likely contribute to PC2 ER localization and function. Overall, this research hopes to contribute information to how PC1 and PC2 traffic and function at cilia.

Acknowledgments

I would like to start this section by expressing my utmost gratitude to my supervisor, Dr. Gagan D. Gupta for taking a chance on me. I am truly grateful for the ways in which you have taught me, challenged me and for the countless hours of guidance throughout my graduate career. I am moving forward with confidence as a result of this incredible journey I have shared with you.

I acknowledge and thank my supervisory and examining committee; Dr. Costin Antonescu, Dr. Andras Kapus and Dr. Michael Olson for sharing their invaluable expertise and support towards my research project.

I want to thank the colleagues and friends I made during my MSc at Ryerson, especially Melissa Iazzi, Sarah Birstonas and Peter Yokhana. Thank for all being amazing friends and most importantly amazing people. Our friendship is one I will forever cherish.

I would like to thank Robert Denning and Shawn McPhadden for providing me with numerous teaching opportunities. Your guidance has taught me a lot about what it takes to be a good teacher and mentor.

Finally, I am very grateful for my family and friends – my parents, Annette and Wayne Brauer, my siblings Hayley and Richard Cosh, my grandmother, Rosalie Rising, my boyfriend, Max Koopman and my best friends, Katrina Barclay and Maddie Iozzi – for their unconditional support during my graduate studies.

Thank you all for making graduate studies so much better in more ways than I can say! I would not be where I am today without all of you.

Table of Contents

List of Tables

List of Figures

List of Abbreviations

aa: Amino acid

ADPKD: Autosomal Dominant Polycystic Kidney Disease

ARPKD: Autosomal Recessive Polycystic Kidney Disease

AP-MS: Affinity purification and Mass Spectrometry

ARL13B: ADP Ribosylation Factor Like GTPase 13B

BioID: Proximity-Dependent Biotinylation For Identification

BirA*: Biotin Ligase

BLOC-1: Biogenesis of Lysosome-Related Organelles Complex-1

BLOC1S2: Biogenesis Of Lysosomal Organelles Complex 1 Subunit 2

BLOC1S6: Biogenesis Of Lysosomal Organelles Complex 1 Subunit 6

BORC: BLOC-One-Related Complex

CD16.7: Fusion of CD6 Extracellular Domain and CD7 Transmembrane Domain

CORVET: Class C Core Vacuole/Endosome Tethering

CTS: Ciliary Targeting Sequence

CTT: Cytoplasmic Carboxy Terminal

ER: Endoplasmic Reticulum

GO: Gene Ontology

HOPS: Homotypic Fusion and Protein Sorting

IP: Immunoprecipitation

INM: Interkinetic Nuclear Migration

MS: Mass Spectrometry

OSBPL8: Oxysterol Binding Protein Like 8

PBS: Phosphate Buffered Saline

PC1: Polycystin-1

PC2: Polycystin-2

PKD: Polycystic Kidney Disease

PKD1: Polycystic Kidney Disease-1

PKD2: Polycystic Kidney Disease-2

PCNT: Pericentrin

PLD: Polycystic Liver Disease

PM: Plasma Membrane

PPI: Protein-Protein Interaction

SAINT: Significance Analysis of INTeractome

SEC63: SEC63 Homolog, Protein Translocation Regulator

SILAC: Stable Isotopes Labeling by Aminoacids in Cell culture

SNARE: Soluble N-Ethylmaleimide-Sensitive Factor Attachment Protein Receptor

SUN1: SUN Domain-Containing Protein 1

SUN2: SUN Domain-Containing Protein 2

SYNE2: Nesprin-2 (Isoform 1)

TGN: Trans Golgi Network

TULP3: TUB Like Protein

1.0 Introduction

1.1 Overview

The development of a protein-protein interaction (PPI) network of the polycystin-1 (PC1) and polycystin-2 (PC2) interface will reveal diverse PPIs that occur during normal polycystin function. It remains unclear how polycystins traffic throughout the cell and how they function. It is likely that other proteins mediate their function, traffic, and are perturbed in the diseased state. Understanding the PPIs of normal functioning PC1 and PC2 will provide information about any interactions that contribute to their function and may be important in our understanding of Autosomal Dominant Polycystic Kidney Disease.

1.2 Polycystic Kidney Disease

Polycystic Kidney Disease (PKD) is an inherited disorder that causes numerous fluid-filled cysts to form and enlarge over a patient's life, ultimately leading to End Stage Renal Disease (ESRD). There are two main classifications of PKD, Autosomal Recessive Polycystic Kidney Disease (ARPKD) and Autosomal Dominant Polycystic Kidney Disease (ADPKD). These two classifications differ in genetic mutation, prevalence, life-expectancy and phenotypic severity. ARPKD is nicknamed 'infantile PKD' as the cystic phenotype arises early in life and impacts approximately 1:20,000 children (Rossetti et al., 2012). It stems from genetic mutation of the PKHD1 gene on chromosome 6p21 with a second locus of mutation in the DZIP1L gene (Smith, 2018). ADPKD is the most common hereditary renal disorder impacting 1:400 to 1:1000 people with the average age of disease onset varying from 20-40 years old, depending on the type of gene mutation (Torres et al., 2007). The cause of renal cyst formation in ADPKD remains unclear.

1.2.1 Autosomal Dominant Polycystic Kidney Disease

ADPKD is distinguished by the pattern and age of onset. Renal cysts can be present from a very young age; however, they largely occur in adulthood. The cause of the disease is from a genetic mutation, but this does not explain why cyst formation is aggressive in adulthood. There are two types of ADPKD: type 1, ADPKD-1 (Chapin & Caplan, 2010), is caused by mutations along the polycystic kidney

disease-1 (PKD1) gene transcript, and type 2, ADPKD-2, is caused by mutations along the polycystic kidney disease-2 (PKD2) gene transcript (Magistroni et al., 2010).

Patients with ADPKD-1 account for about 85 to 90 percent of cases and have an observed life expectancy of about 53 years. Patients with ADPKD-2 have a longer life expectancy of about 69.1 years and account for about 10-15 percent of cases (Wilson et al., 2004). Mutations in either PKD1 or PKD2 have shown to cause ADPKD, but mutations in both lead to earlier and more severe symptoms than those with mutations on only one (Harris et al., 2009). There are hundreds to thousands of mutations determined to contribute to the disease including, missense, point, splice, in-frame/out-frame insertions and deletions, nonsense and frameshift mutations (Audrézet et al., 2012). There is no mutation "hot spot" along either PKD1 or PKD2, as mutations have been reported throughout the gene transcript. As well, less severe mutations such as point mutations, appear to show similar cystic phenotypes as more severe mutations would such as large deletions. Ultimately, the link between mutation and cystogenesis remains unknown.

ADPKD patients exhibit substantial variability in symptoms, especially between the type 1 and type 2. Moreover, interfamilial variation on unique mutations have not be explained. Theoretically, a common mutation should not have different clinical presentations to individuals that share it, however patients have shown that this is not the case. All discovered mutations in PKD1 and PKD2 are stable nucleotide insertions, deletions and substitutions, failing to explain why same or similar family germline mutations exhibit such a large phenotypic variability (Qian et al., 1996). Dizygotic twins with the same nonsense mutation along PKD1 exhibit inconsistent phenotypes (Peral et al., 1996). This could suggest that there are a small number of genetic modifying factors creating phenotypic variability. Examining the PPIs of the mutated and nonmutated genes under different conditions and cells, could shed light on any proteins that contribute to the phenotypic variability.

1.3 Polycystin-1 and Polycystin-2

Polycystins are integral membrane proteins that localize in various places in the cell including the endoplasmic reticulum (ER), plasma membrane (PM) and primary cilium (Ma et al., 2017), however both PC1 and PC2 are thought to have different functions. PC1 is approximately 460 kDa with a large extracellular N terminal, 11 transmembrane domains and a short intracellular C terminal (Figure 1). The function of PC1 remains unclear but is likely a G protein-coupled receptor with various purposes. PC2 is approximately 110 kDa with 6 transmembrane domains and short intracellular N and C termini (Figure 2). The function of PC2 also remains unclear but is likely a non-selective cation channel that is capable of transporting calcium ions (Ca^{2+}) though the ciliary membrane (Anyatonqu & Ehrlich, 2004).

1.3.1 Structure of PC1

PKD1 encodes a large 4303 amino acid (aa) long protein, PC1. The structure consists of a large extracellular N-terminal portion, multiple transmembrane loops and a short intracellular portion. The N-terminal portion harbours: two cysteine-flanked leucine-rich repeats, multiple copies in tandem of a cell-wall integrity and stress-response component homology domain, the first IgG-like repeat, a low-density lipoprotein A domain, a C-type lectin domain, 16 additional IgG-like repeats, a receptor for egg jelly homology domain and a G protein-coupled receptor proteolytic site domain. There are 11 transmembrane domains with a polycystin-1–lipoxygenase-α toxin domain located on the first transmembrane loop on the intracellular side. The C-terminal portion harbours a G-protein binding domain and a coiled-coil domain (Figure 1; Wilson PD, 2004). To date, there are no known domains identified along the other transmembrane loops.

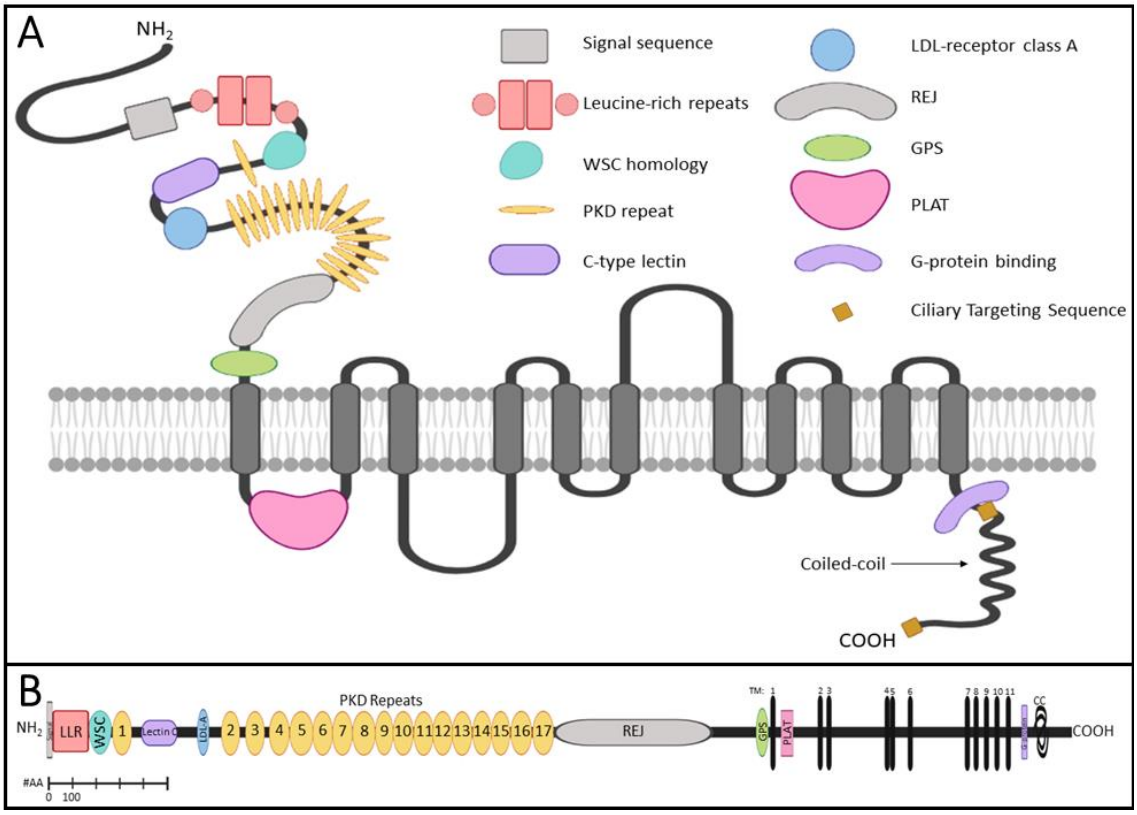

Figure 1. Structure of PC1 domains. Domain positions were obtained from UniProt using the reference number P98161. Illustration was created and edited on BioRender. ***A****: Structure of PC1 with large extracellular N-terminal region, 11-transmembrane domains and a short intracellular C-terminal. Ciliary targeting sequences are illustrated from Zhou et al., 2019 and Ward et al., 2011. Not to scale.* ***B****: Linear representation of the domains along PC1. Amino acid (AA) scale provided, bottom left. Domain positions were obtained from UniProt using the reference number P98161. Illustration was created and edited on BioRender. Signal: signal peptide sequence. LLR: leucine-rich repeats. WSC: cell wall and stress component domain. REJ: receptor for egg jelly domain. GPS: G protein–coupled receptor proteolytic site domain. TM: transmembrane domains, numbered. PLAT: polycystin-1–lipoxygenase-α toxin. G-protein: G-protein binding domain. CC: Coiled-coil domain.*

1.3.2 Structure of PC2

PKD2 encodes a 968 aa long protein, PC2 and commonly called TRPP2, composed of intracellular N- and C-terminal portions with six transmembrane (TM) domains. The PKD2 gene encodes an mRNA transcript containing 15 exons and functions as a Ca^{2+}-permeable non-selective cation channel (González-Perrett et al., 2001). The structure of PC2 shares significant homology to other voltage activated Ca^{2+} channels (Mochizuki et al., 1996). The N-terminal portion is thought to regulate PC2 trafficking through the RVxP motif (CTS) and serine's 76 phosphorylation was found essential for PC2 targeting to cilia (Geng et al., 2006) and PM (Streets et al., 2006). The C-terminal portion harbours: an

EF-hand, ER-retention signal and coiled-coil domain that interacts with PC1. The transmembrane domain between TM5 and TM6 form a channel pore and likely contribute to Ca^{2+} influx (Figure 2). PC2 appears to be dependent on PC1 for channeling Ca^{2+} as well as trafficking to the ciliary membrane (Gainullin et al., 2015).

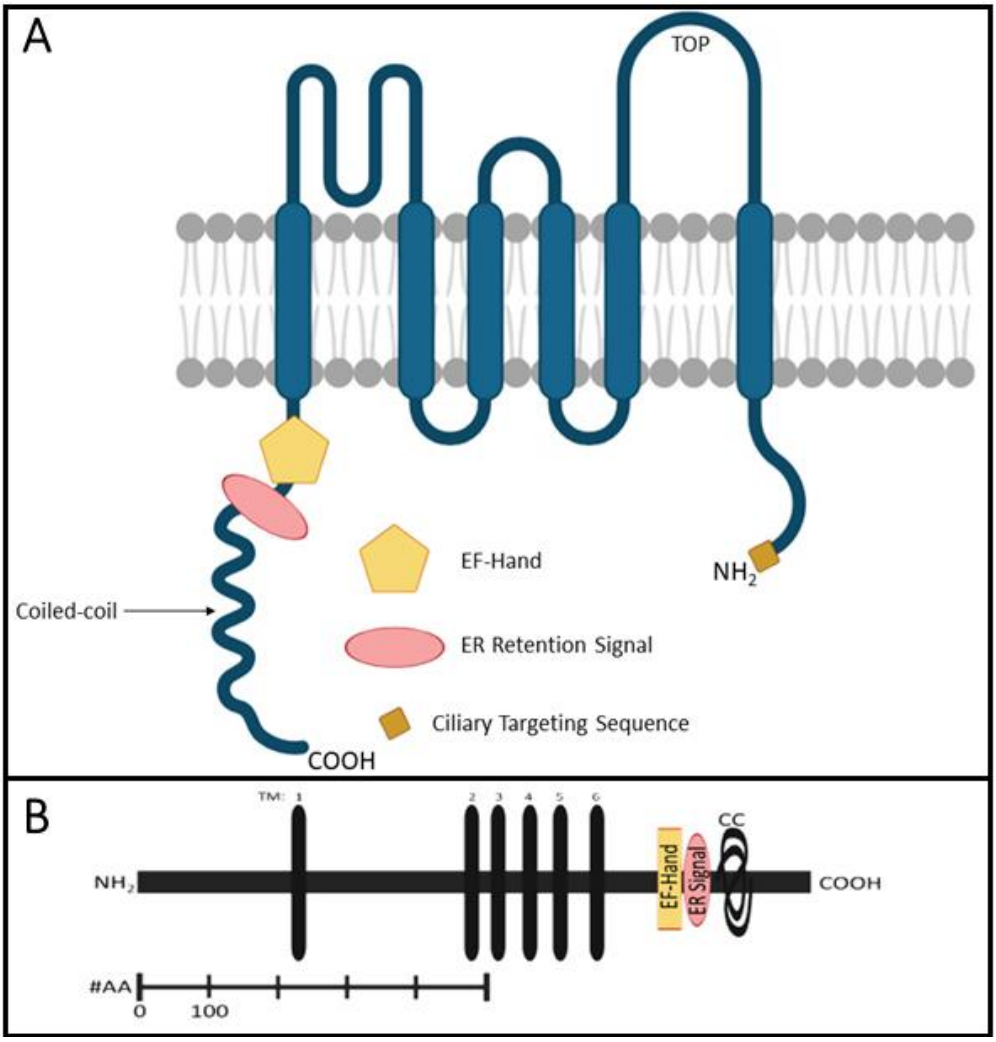

Figure 2 Structure of PC2. Domain positions were obtained from UniProt using the reference number Q13563. Illustration was created and edited on BioRender. Not to scale. ***A****: Structure of PC2 with intracellular N- and C-termini and 6transmembrane domains. Not to scale.* ***B****: Linear representation of the domains along PC2. Amino acid (AA) scale provided, bottom left. Domain positions were obtained from UniProt using the reference number Q13563. Illustration was created and edited on BioRender. CC: Coiled-coil.*

1.3.3 Structure of PC1 and PC2 at Primary Cilia

It is ubiquitously agreed that PC1 and PC2 interact at primary cilium through their cytoplasmic carboxy termini (CTT) and affect cell signaling. Dysregulation of their interaction are extensively shown to lead to ADPKD, confirming that both polycystins must function properly to maintain cellular health. As well, ADPKD causing mutations support the claim that disruption of the PC1/2 complex leads to disease (Su et al., 2018). PC2 appears to be dependent on PC1 for channeling Ca^{2+} as well as trafficking to the ciliary membrane (Gainullin et al., 2015.). Thus, full-length and intact polycystin is critical for the correct function of the PC1/2 complex.

The physical interaction of PC1 and PC2 at the primary cilium is through a coiled-coil domain. This interaction has been confirmed through various methods including a GST pull down (Casuscelli et al., 2009), yeast-two hybrid systems (Qian et al., 1997; Tsiokas et al., 1997) and co-immunoprecipitation assays *in vitro* and *in vivo* (Tsiokas et al., 1997). Structural visualization shows a 1 to 3 stoichiometry of the complex, reporting one PC1 molecule to three PC2 molecules. Mutations in either PKD1 or PKD2 are proposed to impact this complex and/or protein function depending on the mutation type (Qian et al., 1997).

1.3.4 Trafficking Pathways

The major phenotype of ADPKD is renal cysts that arise from mutations where PC1 and/or PC2 fail to correctly localize to cilia. There is accumulating evidence suggesting that PC1 and PC2 ciliary localization is interdependent (Freedman et al., 2013; Gainullin et al., 2015; Kim et al., 2014). Both PC1 (Figure 1) and PC2 (Figure 2) have CTSs that are proven to be essential for ciliary localization, however the targeting mechanisms of PC1 and PC2 are poorly understood.

Protein transport to cilia is convoyed by Golgi-derived vesicles, also termed polarized vesicle trafficking (reviewed by Zeng, 2017). The transport is essential to deliver proteins involved in ciliogenesis and is mediated by small GTPases, which recruit vesicle coating complexes at various stages of

membrane tethering. There are multiple trafficking studies that examine PC1 and PC2 alone, such as Rab/Arf, BBSome and exocyst complexes (Figure 3). However, if the polycystins traffic independently, such experiments would provide insight to at which point the PC1/2 complex is formed.

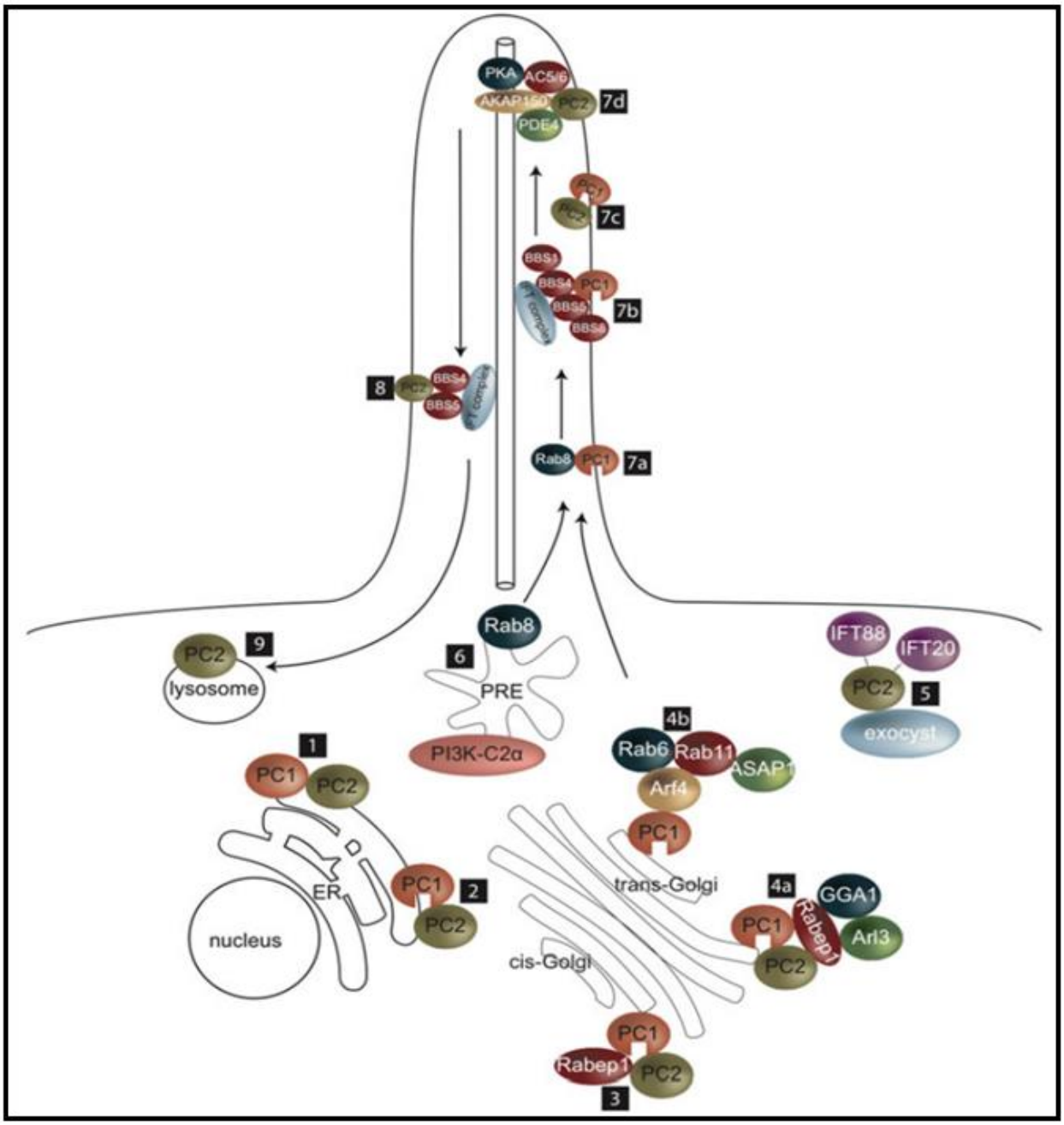

Figure 3. Research behind intracellular trafficking of polycystins, independently and interdependently, to primary cilium through various steps (Miller, 2017). 1) PC1/2 interact in the ER; 2) PC1 is cleaved at the GPS cleavge site; 3) PC1/2 complex interact with GGA1, which binds Rabep1 in pre-Golgi complex; 4) a) Rabep1 binds to GGA1 and Arl3

at the TGN, or; b) PC1 binds Arf4 which bridges interacts with Rab6, Rab11 and ASAP1 in Golgi; 5) PC2 interacts exocyst, in a complex with IFT88 and IFT20, which are responsible for ciliary entry of PC2; 6) PI3K-C2α in the pericentriolar recycling endosome (PRE) activates Rab8 which interacts with PC1 and PC2; 7) a) facilitates ciliary entry of PC1 and PC2, or; b) facilitates ciliary entry of PC1 when BBS1 and the BBsome binds PC1, or; c) PC1 and PC2 enter cilia as a complex, or; d) PC2 is in a complex with AKAP150, AC5/6, PDE4 and PKDA; 8) BBS4 and 5 mediate ciliary PC2 removal, and; 9) PC2 is degraded in the lysosome.

The heterogeneity in localization sequences and targeting pathways in primary cilia are confounding, making it difficult to categorize trafficking of different types of integral membrane proteins into one general model. More recent literature contributes information on the ciliary trafficking of structurally diverse integral membrane proteins mediated by tubby family proteins, TULP3 and found member TUB, as general adapters for ciliary trafficking. Previous G-protein-coupled receptors (GPCRs) were shown to traffic to cilia through TULP3 (Mukhopadhyay et al., 2010). One paper identified numerous integral membrane proteins that undergo TULP3 regulated ciliary trafficking, including PC1 and PC2 (Badgandi et al., 2017). Literature reports that PC1 and PC2 form a complex at the ciliary membrane, however, this research analyzed PC1 and PC2 trafficking as individual ciliary proteins, thus, it remains unclear whether TULP3 mediates PC1 and PC2 traffic as a complex, or individually.

Homozygous mice with a hypomorphic missense mutation in the conserved Tubby domain of TULP3 develop cysts at a late embryonic stage, however, the TULP3 mutation did not impact ciliogenesis (Legué et al., 2019). Additionally, a reduction of PKD1 dosage in the TULP3 conditional mice showed a more severe the cystic phenotype, suggesting a genetic interaction between TULP3 and PC1. This paper also demonstrates that TULP3 is essential for the trafficking of the Joubert syndrome associated small GTPase ARL13B into kidney cilia. It appears that TULP3 plays an important role in controlling distinct ciliary pathways that regulate cystogenesis and could be important our understanding of ADPKD.

Interestingly, conditional deletion of other ciliary genes shows a similar cystic phenotype as the conditional TULP3 mouse, including several IFT complexes (Davenport et al., 2007; Jonassen et al., 2008; Lehman et al., 2008; Jonassen et al., 2012; Tran et al., 2014), and ARL13B (Li et al., 2016; Seixas er al.,

2016). ARL13B is a small GTPase that when mutated, causes the ciliopathy Joubert syndrome. It localizes to the ciliary membrane and likely plays an unknown role in ciliary traffic and assembly (Seixas et al., 2016). ARL13B appears to traffic endocytosed cargo through the endocytic recycling compartment, however its link to cilia has yet to be established (Barral et al., 2012). Additionally, depletion of the exocyst leads to abnormal cystogenesis in 3D cell culture (Zuo et al., 2009). Correspondingly, PC2 is known to be regulated by proteins of the exocyst complex, however its link to ARL13B has yet to be explored (Fogelgren et al., 2011).

Another recent paper discusses a two-step process for PC2 trafficking to cilia (Walker et al., 2019). This was shown using a mouse model carrying a PKD2 mutation that does not impact channel activity but does impacts ciliary localization; the mice experience indistinguishable phenotypes from other ADPKD mice. They showed that the mutant PC2 accumulates at the ciliary base, suggesting that PC2 first traffics to the ciliary base before entry. Additionally, wild-type PC2 appeared to co-localize with the mutant PC2 through a less intense immunostaining (Walker et al., 2019). This paper proposes a new trafficking system of PC2, however modifiers of this pathway have yet to be discovered. Discovering the proteins and modifiers involved in PC1 and PC2 traffic could lead to potential therapeutic targets for ADPKD.

1.4 Primary Cilium

The primary cilium is a minute membrane-encased microtubule-based organelle present in most mammalian cells. It is a sensory organelle that can detect signaling molecules such as Sonic Hedgehog (SHH), transforming growth factor beta (TGF-β), and platelet-derived growth factor (PDGF) (Wheway et al., 2018). It also acts as a mechanosensor that responds to fluid movement, such as that in the kidney (Praetorius et al., 2003). The primary cilium is a nine-doublet microtubule-based organelle anchored to the mother centriole (Venkatesh et al., 2017). The *ciliary membrane* is home to several sensory proteins, receptors, transporters and ion channels that have distinct roles, this is where PC1 and PC2 have been

shown to interact. The *basal body* houses many signaling proteins and is the base to which the ciliary axoneme is rooted to (mother centriole). The *transition zone* connects the basal body and ciliary axoneme, playing a key role in ciliary access and ciliogenesis (Kathem et al., 2014).

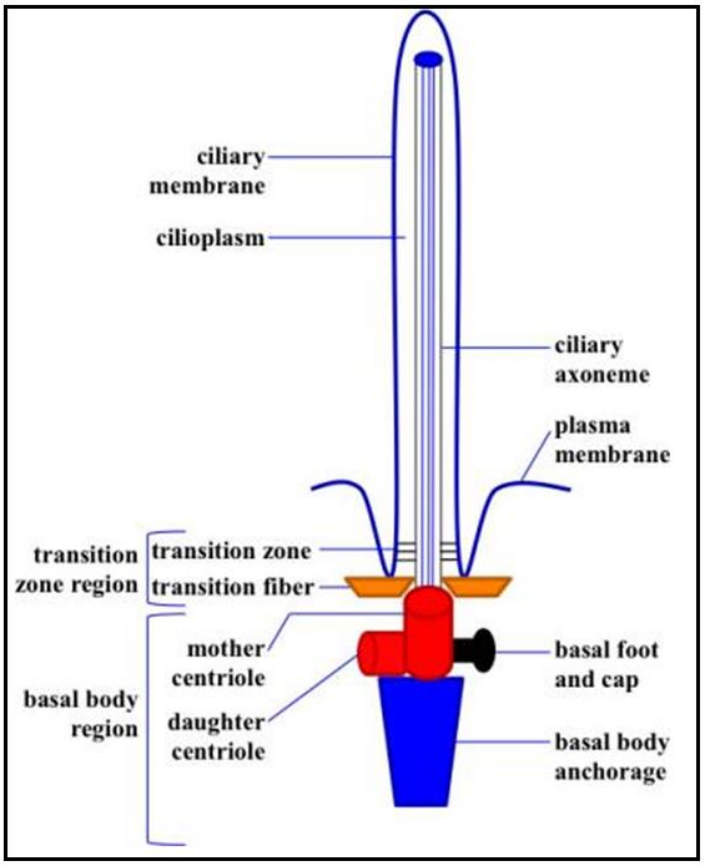

Figure 4. Kathem et al. (2014) show the five main compartments of the primary cilium: the ciliary membrane, the cilioplasm, the ciliary axoneme, the transition zone and the basal body region. The ciliary membrane, cilioplasm and ciliary axoneme protrude from the cell surface, whereas the transition zone and basal body regions can be found settled in the cell.

1.4.1 Ciliopathy

Mutations in the genes expressed in the primary cilia including the cilia anchoring structures, cellular cilia or the basal bodies cause several disorders known as ciliopathies. Since the primary cilium is a component of almost all mammalian cells, ciliary dysfunction causes a variety of abnormal phenotypes. These phenotypes include primarily retinal degeneration, cystic kidneys and cerebral anomalies (Waters et al., 2011). Numerous syndromes have now been grouped under this classification

of ciliopathy including: Bardet-Biedl syndrome, Mechel syndrome, Joubert's syndrome, PKD and many more (Yoder et al., 2007). Although many ciliopathies are caused by defects to proteins that localize in the primary cilium (or motile cilia), it is possible that ciliopathies are also associated with proteins that localize elsewhere but are believed to affect ciliary function through cleavage of ciliary proteins. In ADPKD, the cystic kidney phenotype is a result from either defective ciliary signaling or an inability to assemble cilia.

In the kidney, primary cilia project off the apical surface of the epithelium into the tubule lumen, presenting on most cells of the nephron (Yoder et al., 2007). These primary cilia were first thought to be insignificant for renal development. Nevertheless, studies in model organisms led to an increase in understanding the function of the renal cilium. Although many studies suggest the importance of cilia for normal maintenance of renal physiology, the role and function of the primary cilium, along with its association of cyst formation remains inadequately understood (Kathem et al., 2014). It has been shown that primary cilia were abnormally long in mouse kidney cells associated with cysts after conditional ablation of PKD1 or PKD2, suggesting that these genes could contribute to ciliation and explain how ADPKD is a ciliopathy (Lui et al., 2018).

1.5 Cyst Formation – The Two Hit Model

The 'two-hit' model of cystogenesis in ADPKD recommends that individual cyst formation in ADPKD might involve a secondary factor (Reeders ST, 1992). This model was built analogous to a carcinogenesis model which hypothesizes that two mutational events must occur, either the same gene or another, to cause a phenotypic change (Knudson, 1971). Presumably, the germline mutation is not in itself enough to produce a cyst, so an additional sporadic event, potentially genetic or environmental, is required (Reeders, 1992). The idea behind the two-hit model showcases renal cysts as fluid-filled "tumours", providing a unified model for all PKD patients. The tubular epithelial cells containing a germline mutation of either PKD1 or PKD2 is the initiation of the cyst formation (the first hit). The theory

suggests some sort of external stimuli that assists the initiation (second hit). Therefore, loss of heterozygosity by a somatic mutation, for example, activates the monoclonal proliferation of the cell in which both alleles are inactivated. The cells continuously abnormally proliferate, allowing fluid to flow into the cyst and cause isolated cysts progressively increasing in size (Figure 5; Köttgen et al., 2007). As these cysts increase in size, they constrict important pathways such as blood vessel and blood flow, eventually leading to severe complications and death. It is important to note that there are ciliopathies (Waters et al., 2011) which also result in cystic kidneys, much like ADPKD. By understanding how PKD1 and PKD2 affect cilia formation and maintenance through their interactions with ciliary proteins, we may be able to better understand the mechanism of cyst formation.

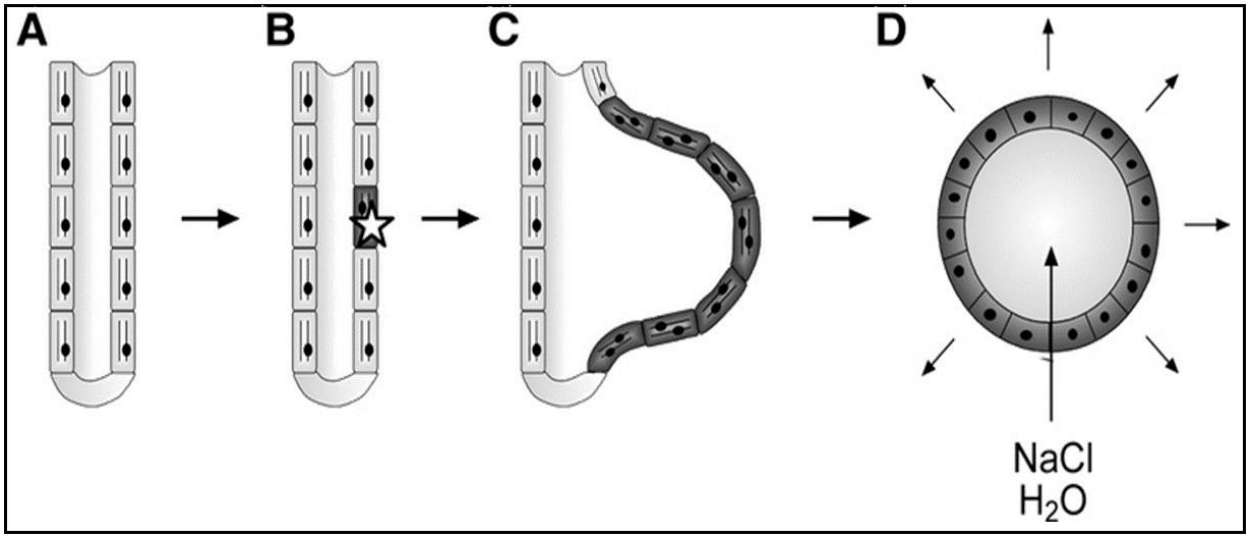

Figure 5. 'Two-hit' model of cystogenesis in ADPKD. a) Cells along the renal epithelium contain the same PKD mutation. b) Somatic mutation of the "WT" PKD allele occur in one of the individual epithelial cells. c) Abnormal proliferation of colonel epithelial cell forms tubular cyst formation. d) Cyst closes off from the renal epithelium and enlarges over time.

A prediction of the 'two-hit' model is that renal cysts will sporadically be found in individuals without any inherited predisposition, but instead stem from the acquisition of two somatic mutations by a single cell. As well, this model also predicts that the number of cysts should increase throughout one's life as second hits are gradually accumulated. It is argued that gradual enlargement of kidneys during

adulthood is a universal feature of the disease, but it is unclear whether change in the number or size of cysts is responsible for the enlargement.

1.6 Proximity Dependent Biotin for Identification

Recently, proximity dependent biotin identification (BioID) has proven to be a powerful technique to study protein-protein interactions specifically in mammalian cells. BioID uses a mutated version of *Escherichia coli* biotin ligase, BirA*, to biotinylate proteins in a live cell within a 10nm radius. The BirA* releases reactive bioAMP, which in turn covalently binds to amines on nearby proteins. This method uses BirA* fused to a bait protein, in this research the bait protein will be either PKD1 or PKD2, to biotinylate proteins, allowing for the creation of a protein interactome. Once biotinylated, cells can be lysed and biotinylated proteins can be recovered by streptavidin affinity purification. Streptavidin and biotin form a strong covalent bond, making it an easy recovery technique. Once the biotinylated proteins are recovered, they are pelleted down and identified with Mass Spectrometry (Varnaité et al., 2016).

The typical labeling period of the BioID method is 24hrs. This is advantageous as it allows for mobility of both the bait and substrate throughout a typical cell cycle. The labeling radius for biotinylation is approximately 10nm for tethered proteins, however the labeling radius may be larger for freely diffusing cytosolic proteins (Kim et al., 2014, Roux et al., 2012). The biotinylated proteins can be enriched using streptavidin beads and identified by Mass Spectrometry (MS). To distinguish between endogenously-biotinylated proteins and those specifically modified through BioID, it is important to include a non-specific control bait that is not fused to the protein of interest, such as cytosolic BirA*.

PC1 and PC2 likely have various functions outside of forming a receptor/channel complex, thus genetic and biochemical approaches for the detection of PPIs are crucial in our understanding of how PC1 and PC2 function and traffic. Such approaches have been used to confirm PC1 and PC2 interactions which include yeast-two-hybrid assays (Gallagher et al., 2000), co-immunoprecipitation (Aguilar et al.,

2017), and high-throughput microarray analysis (Liu et al., 2019). While these techniques have shown to be individually successful, the localization, interactions and activities of the polycystins are diverse. Most of these detection techniques are well suited for detection of interactions that are strong and direct, as well require an understanding of the preys likely to interact with the bait. These techniques also require harsh cell lysis to identify the bait-prey interactions, as well as a prediction of interaction between bait and prey antibody. Misinterpretation of bait antibody can lead to misleading data showing no interacting partner. BioID overcomes these limitations by screening for strong and direct interactions, as well as weak or transient interactions. This technique can screen for previously unknown interactions in a cell's natural context. However, no single method of substrate identification clearly outperforms all others. Comprehensive studies of PKD interactors require the use of orthogonal approaches for identification of interaction partners.

Affinity purification and Mass Spectrometry (AP-MS) is a common technique for the identification of protein interacting partners. However, it has not been widely used to research PKD1 or PKD2. The interactions between the PC1 and PC2 complex are particularly hard to identify due to their transient nature and instability of various isoforms. We used AP-MS in parallel with BioID to study the proximally interacting partners of PC1 CTT and PC2. BioID is suitable for the detection of stable PPIs, however, the permanent nature of biotinylation makes this method useful in the detection of weak and transient interactions. We utilized a proximity-based proteomic approach, BioID, along with traditional AP-MS to discover new PKD associated interactions or modifiers that may contribute to a fuller understanding of polycystin function and traffic throughout a full cell cycle. This marks the first use of this methodology to the study PC1 and PC2 interactors.

There have been recent large-scale studies determining the PKD1 interactome (Nigro et al., 2019) and transcriptome (Cai et al., 2018), however none yet have been completed using BioID nor focused on the membrane bound CTT. The first PC1 interactome was completed using a SILAC/MS

approach where the authors identified binding partners of tagged endogenous PC1. Mouse embryonic fibroblasts from a PKD1HA/HA mouse model were used, in which an in-frame HA-tag is incorporated along the last exon of PKD1. This HA-tag allowed for immunoprecipitation (IP) of the endogenous protein. Two IP approaches were taken using a Stable Isotopes Labeling by Aminoacids in Cell culture (SILAC) including in-gel protein digestion and digestions directly on the beads. These two approaches were completed because while soluble proteins are better digested in solution, membrane proteins, such as PC1 are better digested if completely denatured in the gel (Nigro et al., 2019). This shows the limitation to the technique when comparing it to AP-MS, where the streptavidin-biotin affinity is very strong and occurs in a single step of the protocol. Additionally, the authors detected a class of interactors mediating regulation of cellular actomyosin contraction that negatively regulates cellular contraction and YAP activation in response to extracellular stiffness.

The PKD1 transcriptome research presented similar results using a kinase inhibitor screen on a 3D cell culture of PKD1 mouse mutant cells (Cai et al., 2018). This method used data from gene profiling on human PKD1 cysts compared to minimally cystic tissues using Affymetrix cDNA arrays (Song et al., 2009), because presented transcriptional profiles characteristic of differentiation genes and reactivation of developmental and mitogenic signaling in ADPKD tissues. Using almost 400 direct YAP/TAZ target genes, it was determined that most were significantly enriched in ADPKD cysts, showing YAP/TAZ and transcriptional targets to be critical mediators of cyst kidney pathogenesis (Cai et al., 2018). However, this research used IMCD3 cells, which can have different gene transcripts compared to human cells. As well, this research studied gene transcripts instead of functional proteins, making it hard to compare to this thesis research on PPI. Overall, the interactome and transcriptome do not overlap with the BioID completed in this research as it focuses on the adverse effects of PC1 CTT cleavage function and YAP/TAZ nuclear translocation. This research focuses on membrane bound PC1 CTT, as well as how it traffics throughout the cell.

2.0 Overview and Hypothesis

The PKD1 and PKD2 gene encodes for the PC1 and PC2 proteins respectively. PC1 and PC2 interact at primary cilia to form an intracellular complex through a coiled-coil domain along their C-termini. Mutations in either PKD1 or PKD2 impact their ability to localize to cilia, form a complex and lead to an inherited monogenic disorder termed ADPKD. ADPKD is a genetic disorder that causes cysts for form on the kidney and enlarge over a patient's life. Unfortunately, this leads to end-stage renal failure, impacting 1:400-1:1000 North Americas on average (Gonzalez-Parrett et al., 2001). Neonatal renal cysts can occur; however, cysts generally form and grow more rapidly in later decades of life. As this disease progresses, renal cysts compress surrounding parenchyma and cause renal failure. Currently treatments for the disease is generally dialysis or transplant, there is no cure.

Proximity dependent biotinylation for identification (BioID) is a protein-protein interaction technique used specifically in mammalian cells. BioID uses a mutated biotin ligase from *Escherichia coli*, BirA, to biotinylate proteins in close proximity. BirA can be fused onto a bait protein of interest, and in the presence of biotin, will biotinylate endogenous proteins within a 10 nm radius (Kim et al., 2014). The biotinylated proteins can be identified through MS. This approach can not only identify direct interactions, but also weak and/or transient interactions in live cells.

Our understanding of the protein interactions associated with the PC1 and PC2 C-terminal coiled coil complex is poor. It is also ill understood how this domain is connected to primary cilia. It is likely that interacting proteins are associated with polycystin function and may be important in our understanding of ADPKD. By examining the interactions along the coiled-coil domain, we will be able to determine if there are any key proteins that contribute to the disease. We hypothesize that one or more of the interactions may be perturbed in the diseased state, thus investigating how the PKD C-terminal coiled-coil domain interactome changes upon mutation may provide better insight to disease treatment or cure.

3.0 Rationale

Lack of PC1 or PC2 at primary cilia leads to the clinical features of ADPKD, however, how polycystin traffic to cilia remains unknown. Research suggests that presence of both PC1 and PC2 is required for proper localization and function. For example, PC2 does not translocate to cilia in the absence of PC1 (Freedman et al., 2013). In addition, PC2 does not exhibit cation channel activity in the absence of PC1 (Xu et al., 2003). Finally, mutations in either PKD1 or PKD2 result in the same cystic phenotype (Wu et al., 2002). For these reasons, we believe the PC1 PC2 coiled-coil complex is a crucial interaction for polycystin trafficking, function and overall cell health. It is likely that screening the protein-protein interactions of the PC1 PC2 complex will reveal novel interactors that mediate polycystin traffic and function at primary cilia. Understanding how PC1 and PC2 function at primary cilia could provide insight to understanding why they are important in disease mechanism and cyst formation.

4.0 Experimental Procedures

4.1 Generate PKD Constructs

In order to examine the genes of interest, PKD1 and PKD2, two cloning techniques were used: Gateway™ cloning for PKD2 constructs, and PCR cloning for PKD1 constructs.

Gateway™ cloning is a method that transfers DNA-fragments between plasmids using specialized “att” sites and the LR Clonase™ enzyme mix. PKD2 was ordered as a Gateway entry clone and has been successfully cloned into the N-terminal GFP and BirA vectors. Several attempts were made to clone PKD2 into the C-terminal BirA vectors, both through Gateway cloning and enzyme-less cloning, with all being unsuccessful. The PKD2-BirA fusion construct cloning was externally completed by Bio Basic Canada Inc.

The NEB HiFi DNA Assembly is a one-step enzyme-less cloning method that was used for PKD1 cloning. It allows for seamless assembly of multiple DNA fragments without the use of restriction enzymes. In order to complete this cloning technique, primers were designed that overhangs from the entry vector, PKD1, to the destination vector, BirA. These primers were used to amplify PKD1 at the appropriate annealing and extension temperatures. Since the primers were very guanine-cytosine rich, it was expected to see primer-dimer reactions after the PCR. The first PCR trial had several primer-dimers, so an enhancer was added to the reaction. Then, the destination vector was cut using two restriction enzymes, HindIII and NotI so that the primers from amplified DNA would attach to the linearized destination vector, BirA. The overlap regions were joined via the Assembly Master Mix, after which the reaction products were transformed into DH5α competent cells, grown, purified and validated using sanger sequencing.

4.2 Cell Culture

hTert RPE-1 cells were cultured in Dulbecco’s Modified Eagle Medium and Ham’s F-12 Medium (DMEM:F12, ATCC), supplemented with 2mM L-glutamine, 1% penicillin streptomycin and 10% fetal

bovine serum (FBS, ATCC). HEK 293 T-REx FlpIN cells were cultured in High-Glucose DMEM (ATCC) supplemented with 2mM L-Glutamine, 1% penicillin streptomycin and 10% FBS (ATCC). Passaging both cell lines once ~90% confluent, cells were washed once with 10mL PBS and trypsinized with 0.25% trypsin-EDTA, incubated for 1-5 minutes until all cells detached and then reintroduced to the recommended media. To induce ciliation, the recommended media was supplemented with 0.5% FBS instead of 10% FBS, and incubated for either 24hrs, hTert RPE-1, or 48hrs, HEK 293 T-REx FlpIN. All cell lines were grown at 37^{o}C in 5% CO_2.

4.3 Transient Transfection of hTert RPE-1 Cells

The RPE-1 hTert cell line is an immortalized line which was used for transient transfection as they have a high transfection efficiency and ciliate well. One day prior to transfections, cells were seeded in a 12-well cell culture plate on 10mm coverslips at a density of 100,000 cells per well. Cells were approximately 75-80% confluent upon transfection. The transfected DNA was used at a concentration of 0.8µg in 50µL Opti-Minimal Essential Medium (Opti-MEM, Reduced-Serum Medium, Gibco). The transfection reagent, Lipofectamine 2000, was used at a 1.2µL in 50µL Opti-MEM. The diluted transfection reagent and DNA were mixed and incubated at room temperature for 20 minutes then added dropwise to the seeded cells. After 16-24 hours, the DNA has successfully transfected into the cells and can either be fixed or induced to ciliate. Cells that are transfected with BirA constructs were fixed with ice cold methanol for 10 minutes, whereas cells that are transfection with GFP constructs were fixed with 4% PFA for 10 minutes.

4.4 Generation of Stable Cell Lines

HEK293T-REx cells are a tetracycline-inducible system incorporating the Flp-IN system. The Flp-IN system allows for DNA to be integrated into the genome at the same locus in each cell, therefore reducing the chance of spurious integration events. Located on each of the PKD constructs are Flp Recombination Target sites (FRT sites) that are linked to hygromycin resistance. The PKD constructs

were co-transfected with pOG44, which mediates integration of the vector into the genome through the FRT site via expression of the Flp recombinase (Ward et al., 2011). Transiently transfected cells are commonly used, however there is often differences in expression levels among the transfected population. Using the FlpIN system to create stable cell lines is advantageous as it removes possible variation in expression levels due to its specific site of integration into the chromosome of the gene, as well as allowing cells to be grown without expression of the transfected protein of interest until such time is required. The tetracycline-inducible system ensures the gene expression is controllable via the addition of tetracycline to the media, so that the chance of over-expression related artefacts is reduced. This cell line is stably expressing the tet repressor (TREx) protein which prevents transcription in the absence of tetracycline by binding to the Tet operator region in the promoter of the PKD vector.

The following constructs were stably expressed in HEK 293 T-REx Flp-IN cells (Supp. Figure 3): BirA-PKD2, PKD2-BirA, GFP-PKD2, CD16.7-PKD1-BirA, CD16.7-BirA and FLAGBirA. One day prior to transfections, cells were seeded in a 6cm plate at a density of 800,000 cells. Cells were approximately 75-80% confluent upon transfection. The transfected DNA was used at a concentration of 1µg, and pOG44 was used at a concentration of 2µg, in 50µL serum-free DMEM. The transfection reagent, Polyjet™ was used at 3µL in 50µL of serum-free DMEM. The diluted transfection reagent, DNA and pOG44 were mixed and incubated at room temperature for 10-20 minutes then added dropwise to the seeded cells. The next day, the media was replaced with 5mL of the recommended media. The following day, the transfected cells were selected using 400µg/mL hygromycin b. The media was changed every four days until colonies were confluent enough to split into a 10cm plate.

4.5 Immunofluorescence

Cells were fixed either in ice-cold methanol (BirA constructs) or 4% PFA (GFP constructs) for 10 minutes. PFA fixation required an additional permeabilization for 10 minutes with 0.3% Triton X-100 in PBS at room temperature. After fixation and/or permeabilization, cells were incubated in a wash and

blocking solution of 0.05% Tween 20, 1% BSA and 10% PBS for 10 minutes. Cells were incubated for 30 minutes at room temperature with primary antibodies diluted to the recommended amount. Cells were washed three times with PBS and incubated for 30 minutes at room temperature with secondary antibodies, DAPI and sometimes Streptavidin HRP 488, all diluted to the manufacturer's recommendation. Cells were washed three times with PBS and mounted to glass slides with mounting media. Visualization of the stained cells was completed at 60X on either the EVOS M7000 microscope or DeltaVision Elite Deconvolution microscope.

4.6 Immunoblotting

Cells grown in a 6-well plate were incubated with 400uL of Mammalian Protein Extraction Reagent (M-PER) and gently agitated at room temperature for 5 minutes. The cell lysate was spun down to pellet the cell debris with the supernatant transferred into a new tube. The solution was lysed further in 400uL of 1x Laemmli SDS-sample buffer (Supp. Figure 7). The samples were separated by SDS-PAGE and transferred, via a semi-dry transfer, to nitrocellulose membrane. Immunoblotting was performed with antibodies in 3% skim milk and 0.2% Tween-20, diluted to the manufacturer's recommendation. The diluted primary antibody solution was incubated overnight at 4^{o}C while being gently agitated. The diluted secondary antibody solution was incubated for 45 minutes at room temperature while being gently agitated. Between each incubation step, the membrane was vigorously washed. For protein detection, an Enhanced Chemiluminescence (ECL) mixture was placed on the membrane for 5 minutes and then imaged using a ChemiDoc™ imaging system.

4.7 BioID and Mass Spectrometry

Cells stably expressing the cloned constructs were split into two replicates, each with a ciliated and non-ciliated sample, and expanded to five 15cm plates. Each sample must reach approximately 80-90% confluency before prepared for BioID. There are approximately 20.0 x 10^6 cells in a 15cm upon confluency, thus each BioID sample contained approximately 100,000,000 cells.The cells were induced

for 24 hours with 1mM tetracycline and 50mM biotin, which is sufficient for expressing the bait of interest and biotinylating endogenous proteins. The cells were scraped, spun down, and stored at -80^{o}C until ready to be processed for MS. The cells were maintained on ice during the scraping process. Cells were gently scraped and placed into 50mL chilled falcon tubes and centrifuged at 15000rpm for 5 minutes. The excess media was decanted, and the pellet was resuspended in 10mL chilled PBS. 100µL from each sample is set aside in centrifuge tubes for western blot validation. The resuspended pellet was centrifuged for three minutes at 1600rpm. The excess PBS was decanted, and the pellet was placed in -80^{o}C for storage.

Preparing the cell samples for MS requires cell lysis and purification using streptavidin. The lysis was completed by incubating the samples in RIPA buffer at 4^{o}C gently agitating for 1 hour, and then sonicating. The samples were then washed with Streptavidin-Sepharose beads (GE ref#17-5113-01) to pull down any biotinylated proteins. The beads were washed vigorously to detach non biotinylated proteins from the beads. Digest the biotinylated proteins with trypsin for 2 or more hours at 37^{o}C in a water bath to remove them from the beads, transferring the supernatant to another tube. Dry the sample with a Speed Vacuum overnight and complete MS. The MS was completed by Dr. Jonathan St-Germain in collaboration with Dr. Brian Raught.

4.7.1 Data Analysis

Upon completion of MS, the results are uploaded to http://142.1.32.46/Prohits/ where the data was extracted. Prohits 4.0 is an open source software package hosted by the Lunenfeld-Tanenbaum Research Institute designed to store, search and analyze MS data. Each of the sample reports were viewed unfiltered, including contaminants as well as true interactors. All samples were then subjected to Significance Analysis of the INTeractome (SAINT). SAINT analysis is a tool for assigning confidence scores to PPIs based on quantitative proteomics data in AP-MS experiments. It converts the spectral count of a prey protein identified in a purification of bait into the probability of true interaction between the

proteins (Choi et al., 2011). The controls, Flag-BirA and BirA-Flag were used to determine non-specific interactions, as well as interactions specific to the Flag-tag or the BirA*. The control CD16.7-BirA was not treated as a control in the SAINT analysis, however it was compared further to the CD16.7-PKD1-BirA data. SAINT score of ≥0.9 was applied to the protein-protein interaction (PPI) data as it corresponds to a false discovery rate (FDR) of 1% (Choi et al., 2011). Therefor, all preys are considered to proximally interaction with the bait with >90% statistical confidence.

5.0 Results

5.1 Construct cloning

PKD1 and PKD2 vectors were cloned into a BirA vector with a FLAG-tag to create PKD-fusion constructs for BioID. Each construct was confirmed by either restriction digest, sequencing or both. The constructs were validated using immunofluorescence in a model ciliated cell line, hTert RPE-1 (Supp. Figure 4). For the PKD1 fusion construct, a chimeric portion that included the last 112 aa of PKD1 was used whereas full-length PKD2 was used. These constructs were used in future experiments, such as BioID and localization experiments in other cell lines.

5.1.1 CD16.7-PKD1-BirA

The PKD1 fusion construct, termed CD16.7-PKD1-BirA from now on, is a chimeric fusion protein which includes extracellular CD16 domain, transmembrane CD7 domain, the last 112 aa of PKD1 and BirAFLAG. The CD16.7-PKD1 construct was gifted to us by Dr. Seth Alper in pcDNA4 (Chernova et al., 2005). This construct mimics the PC1 CTT as it has been demonstrated in multiple research papers to mimic the function of the PC1 CTT as it localizes like full-length PC1 and allows for interaction with PC2 (Arnould et al., 1998; Kim et al., 1999; Kim et al., 1999). It was previously shown to interact with PC2 CTT, like full-length PC1 would, demonstrated by a yeast-two-hybrid assay (Tsiokas et al., 1997). Another paper showed how the chimeric PC1 CTT fusion construct was able to mediate normal PC2 function as a Ca^{2+} permeable cation channel in a similar manner as full-length PC1. The paper compared the absence of PC1, full-length PC1 with the chimeric PC1 CTT (CD16.7-PKD1) and showed that the chimeric fusion protein was able to increase the magnitude of nominally endogenous Ca^{2+} permeable cation currents (Vandorpe et al., 2001). Additional experiments by the same authors showed the similarity, specificity and relevance of the currents of chimeric PC1 CTT to the physical function of intact PKD1 (Vandorpe et al., 2002). These authors also developed patient missense mutations that abolishes the previously shown cation current. These constructs were also graciously gifted to us by Dr. Seth Alpter in pcDNA4 and will likely be used in future experiments (Chernova et al., 2005). These findings reinforce the

physiological relevance of the CD16.7-PKD1 CTT to the function of intact PKD1 in cell culture. Therefore, we chose to use this chimeric construct as we wanted to simplify the interpretation of the BioID to the PC1 CTT.

A fusion cloning strategy was employed to generate the CD16.7-PKD1-BirA construct (Figure 6A). The cloning process started with the creation of primers for PKD1 which included overhands matching the insertion site to BirAFLAG desintation vector (Figure 6B). The PKD1 portion was PCR amplified and purified from the gel and used in the DNA assembly (Figure 6C). The vector backbone, BirAFLAG, was linearized with HindIII and NotI leaving an overlapping region that could be joined using enzyme-less assembly (Figure 6D). Digested products were purified and ligated. The entire insert was verified by sanger sequencing.

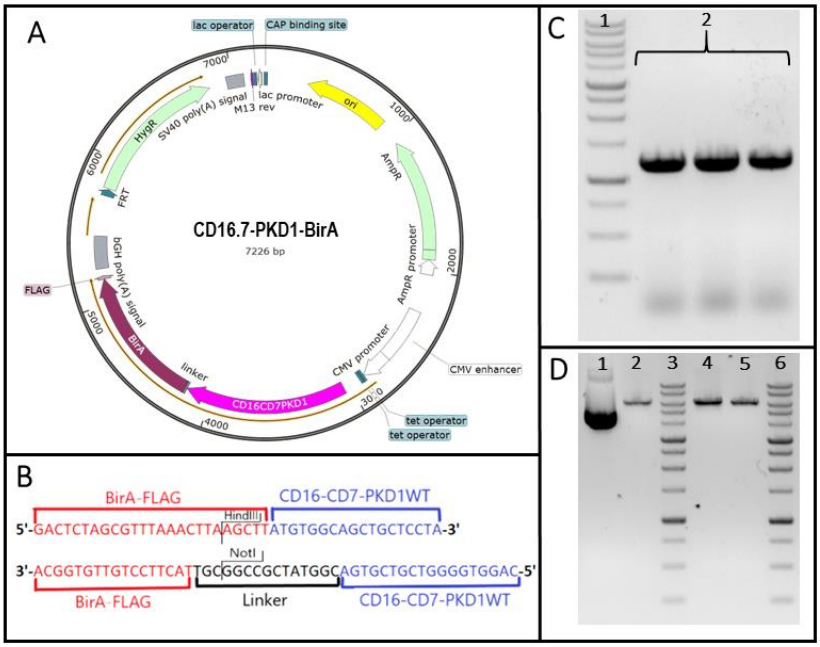

Figure 6. CD16.7-PKD1-BirA Construct Cloning and Validation. ***A****: Virtual cloning completed via http://nebuilder.neb.com including CD16.7-PKD1 in pcDNA5_FRT-TO[MCS]BirAFLAG. Sequence was copied into SnapGene.* ***B****: Primers created on http://nebuilder.neb.com overlapping in pcDNA5_FRT-TO[MCS]BirAFLAG (red) and CD16.7-PKD1-WT (blue). The vector backbone was digested with HindIII and NotI.* ***C****: Successful Polymerase Chain Reaction amplification of the primers from* ***B*** *with minimal primer-dimers. Lane 1: 1kb Ladder. Lanes 2:*

Amplified PCR product. 10mM dNTPs, 10µM forward primer, 10µM reverse primer, template DNA (CD16.7-PKD1), Q5 High-Fidelity DNA Polymerase, Q5 High GC Enhancer and Nuclease-Free Water. ***D****: 1% agarose gel electrophoresis restriction enzyme digest of pcDNA5_FRT-TO[MCS]BirAFLAG plasmid using CutSmart NEBuffer, heat inactivated at 80°C for 20 minutes. Lane 1: Un-cut BirA-FLAG. Lane 2: BirA-FLAG cut with HindIII. Lane 3: 1kb Ladder. Lane 4: BirA-FLAG cut with NotI. Lane 5: BirA-FLAG cut with HindIII and NotI. Lane 6: 1kb Ladder.*

5.1.2 BirA-PKD2

To get a representation of the interactome of intracellular N-terminal portion of PC2, BirA was fused to full-length PKD2. Cloning of the BirA-PKD2 fusion construct was completed via Gateway™ Cloning (Figure 7A). The cloning included an entry vector, pEntry PKD2, a destination vector, pDest FLAGBirA and an enzyme mix, LR Clonase™, that catalyzes the recombination between the two vectors. After cloning, the fusion construct was validated using restriction enzyme digests and sanger sequencing. The cut sites matched the predicted size of BirA-PKD2 (Figure 7B). Immunofluorescence was completed to confirm expression and to determine localization. An additional fusion construct that was fluorescently tagged was cloned via Gateway™ Cloning to supplement localization data. The fusion construct, GFP-PKD2, coincided with the localization data of BirA-PKD2 (Supp. Figure 1; Supp. Figure 5).

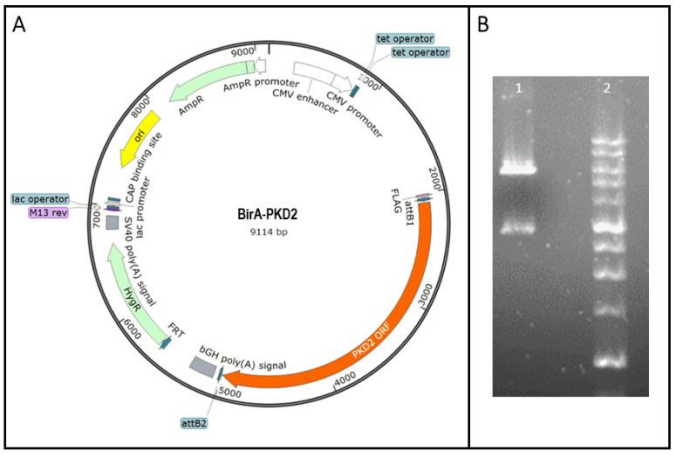

Figure 7. BirA-PKD2 Construct Cloning and Validation. ***A****: Virtual gateway cloning completed via SnapGene including PKD2 Gateway Entry clone V94950 in V8164 pcDEST-BirA-Flag-N-Ter.* ***B****: 1% agarose gel electrophoresis confirmation of V8164 pcDNA5-pcDEST-BirA-Flag-N-Ter PKD2 Gateway Entry via restriction enzyme digest using HindIII and CutSmart NEBuffer at 50% activity, heat inactivated at 80°C for 20 minutes. Lane 1: NBirA-PKD2 via Gateway cloning. Lane 2: 1 kb Ladder.*

5.1.3 PKD2-BirA

To get a representation of the interactome of intracellular C-terminal portion of PC2, BirA was fused to full-length PKD2. The fusion cloning strategies for PKD2-BirA, Gateway™ Cloning and enzyme less cloning, were unsuccessful (Supp. Figure 2). The PKD2-BirA construct was externally cloned by Bio Basic Canada Inc (Figure 8A). The fusion construct was validated using restriction enzyme digests and sanger sequencing. The cut sites matched the predicted size of PKD2-BirA (Figure 8B). Immunofluorescence was completed to confirm expression and to determine localization.

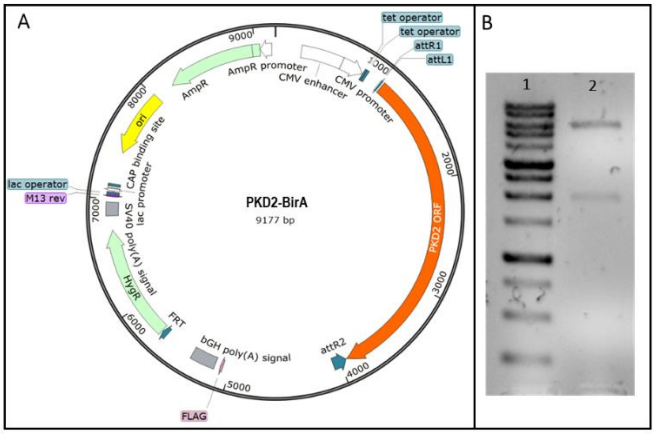

Figure 8. PKD2-BirA Construct Cloning and Validation. ***A****: Cloning completed by Bio Basic Canada Inc., sequenced and copied into SnapGene including PKD2 Gateway Entry clone V94950 in V8449 pDEST-BirA-Flag-C-ter.* ***B****: 1% agarose gel electrophoresis confirmation of PKD2 Gateway Entry V8449 pDEST-BirA-Flag-C-ter via restriction enzyme digest using HindIII and CutSmart NEBuffer at 50% activity, heat inactivated at 80°C for 20 minutes. Lane 1: 1kb Ladder. Lane 2: PKD2-BirA.*

5.2 PKD-Causing Mutations

There is a lot of variability among the PKD-causing mutations. Mutations are found throughout the gene transcript and can be either truncating or non-truncating. There is no mutation "hot spot" along either PKD1 or PKD2. As well, less severe mutations, such a point mutation, appear to have the same cystic phenotype as a large deletion would. This suggests that mutations eventually alter the final exon which contains the interaction sequences between PC1 and PC2. Currently, there are thousands of sequence variants of the PKD1 and PKD2 gene reported in the ADPKD Mutation Database (PKDB)

(http://pkdb.mayo.edu; last accessed August 2019). The sequence variants were compiled and visualized to demonstrate variability.

5.2.1 PKD1

The PKD1 sequence variants were compiled by graduate student, Dhairya Patel. From 2080 unique pedigrees, there are 2323 sequence variants of the PKD1 gene (Figure 9A). Most sequence variants are substitutions, frameshift or nonsense mutations (Figure 9B).

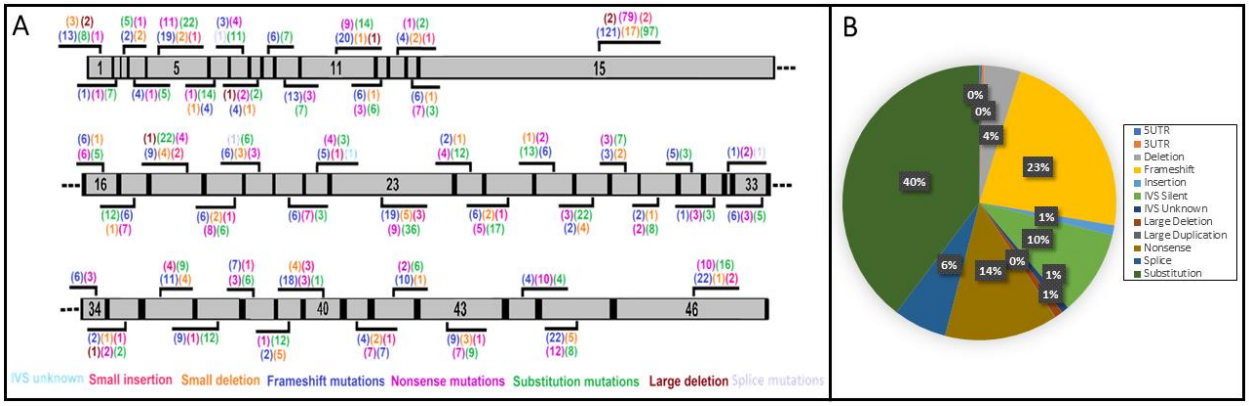

Figure 9. PKD1 Sequence Variants. All data was collected from http://pkdb.mayo.edu, last accessed August 2019. ***A****: Dhairya Patel illustrated the distribution of mutation types found along the PKD1 transcript. The legend is at the bottom coloured to correspond with the type of mutations. The coloured numbers represent the amount of sequence variants along each exon.* ***B****: I created a chart to show the variety of mutations that* ***A*** *exhibits.*

5.2.2 PKD2

I compiled the PKD2 sequence variants. From 463 unique pedigrees, there are 278 sequence variants from the PKD2 gene (Figure 10A). Like the PKD1 mutations, PKD2 exhibits mainly insertion, nonsense and splice mutations (Figure 10B).

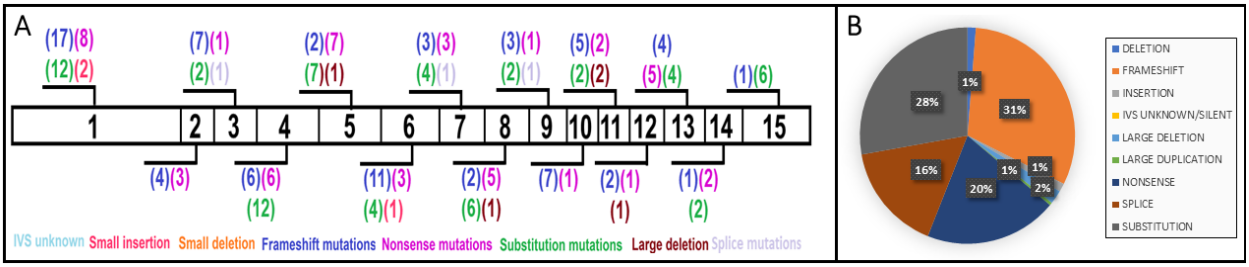

Figure 10. PKD2 Sequence Variants. All data was collected from http://pkdb.mayo.edu, last accessed August 2019. ***A****: The distribution of mutation types found along the PKD2 transcript. The legend is at the bottom coloured to correspond with the type of mutations. The coloured numbers represent the amount of sequence variants along each exon.* ***B****: A chart to show the variety of mutations that* ***A*** *exhibits.*

5.3 Generation of Stable Cell Line

5.3.1 Generation of Stable CD16.7-PKD1-BirA HEK293 T-REx Cell Line

The CD16.7-PKD1-BirA plasmid was transfected into the HEK293 T-REx cell line, validating localization through immunofluorescence and confirming expression by western blot. The fusion protein was validated through immunofluorescence to localize mainly at the cell's membrane (Figure 11A). It did not appear to localize at primary cilia in most cells, however some were identified to have faint expression of the fusion protein (Figure 11B). Biotinylation was validated using a fluorescent Streptavidin probe, which showed co-localization with the fusion protein (Figure 11A). The fusion protein (~87kDa) was expressing at the correct size (Figure 11C; Supp. Figure 10). Both immunofluorescent and western blot experiments were performed with positive and negative controls and with and without tetracycline induction.

Since only a chimeric PC1 CTT construct was being used, we were worried that having a cytosolic BirA control would not account of BirA specific interactions at the PM or cilia. As well, we were worried that there would be CD16.7 specific interactions that we could mistake for PC1 interactions during BioID. To combat this, we created a CD16.7-BirA construct. This construct was stably expressed in the same cell line and its expression was validated (Figure 11D & 11E).

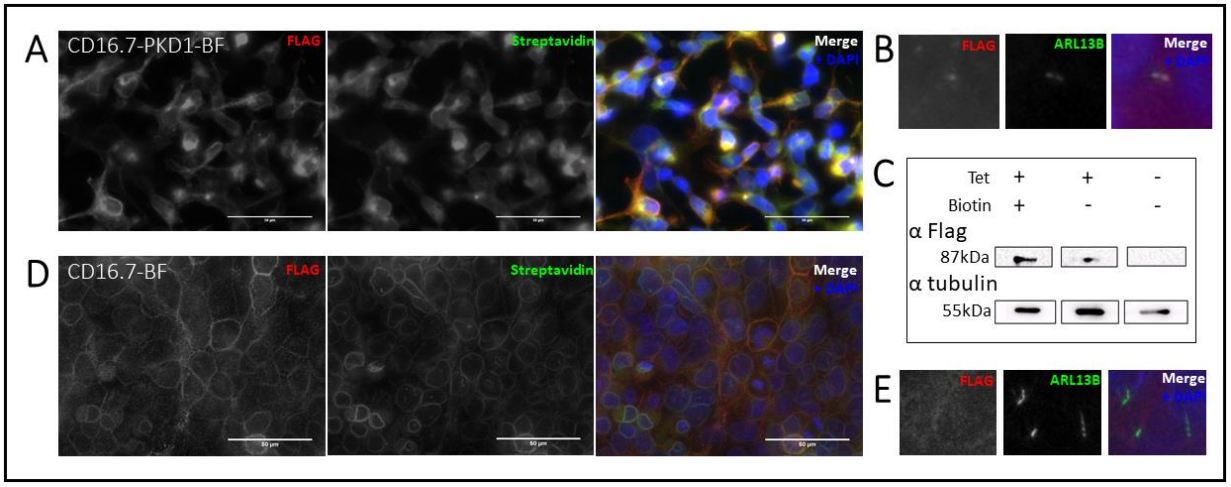

Figure 11. CD16.7-PKD1-BirA Validation. ***A-B****: Stably expressing CD16.7-PKD1-BirA in HEK 293 T-REx cells were subjected to immunofluorescence (IF) staining to visualize cellular localization of PKD1 using anti-FLAG, to confirm*

biotinylation using a Streptavidin probe and to confirm co-localization with ciliary marker ARL13B using anti-ARL13B. ***C****: Western blot validation of CD16.7-PKD1-BirA fusion protein expression.* ***D-E****: Stably expressing CD16.7-BirA in HEK 293 T-REx cells were subjected to immunofluorescence (IF) staining to visualize cellular localization of PKD1 using anti-FLAG, to confirm biotinylation using a Streptavidin probe and to confirm co-localization with ciliary marker ARL13B using anti-ARL13B. (BF: BirAFLAG)*

5.3.2 Generation of Stable PKD2-BirA and BirA-PKD2 HEK293 T-REx Cell Lines

Each plasmid, PKD2-BirA and BirA-PKD2, were transfected into the HEK293 T-REx cell line independent of each other to create two stable cell lines. Localization was validated through immunofluorescence and expression was confirmed by western blot. The fusion proteins were validated through immunofluorescence to localize mainly at the ER (Figure 12A, 12C & 12F). They did not appear to localize at primary cilia or PM as anticipated (Figure 12B & 12I). HEK293 T-REx express endogenous PKD1 and PKD2 at low levels, so perhaps the overexpression of PKD2 requires a higher level of PKD1 expression to traffic to the cells surface. Biotinylation was validated using a fluorescent Streptavidin probe, which showed co-localization with the fusion protein (Figure 12F). For PKD2-BirA, endogenous PKD2 levels were shown in comparison to exogenous levels using a PC2 antibody (Figure 12C & 12D). For BirA-PKD2, biotinylation was also confirmed through western blot using a Streptavidin antibody (Figure 12H). The fusion proteins (~150Da) were expressing at the correct size (Figure 12D, 12G; Supp. Figure 8; Supp. Figure 9). All immunofluorescence and western blot experiments were performed with positive and negative controls and with and without tetracycline induction.

Full-length PC2 was used during the BioID experiments, unlike the chimeric PC1 fusion protein CD16.7-PKD1-BirA. We anticipated that several protein-protein interactors were going to specifically interact with BirA. To combat this, we stably expressed a BirAFLAG vector into the same cell line and validated its expression. Instead of using a targeted BirA vector, such as targeting it to the ER, we chose to use cytosolic BirA as a control (Supp. Figure 6). We did not want to negate any ER related interactions that could be crucial in membrane protein folding and/or trafficking.

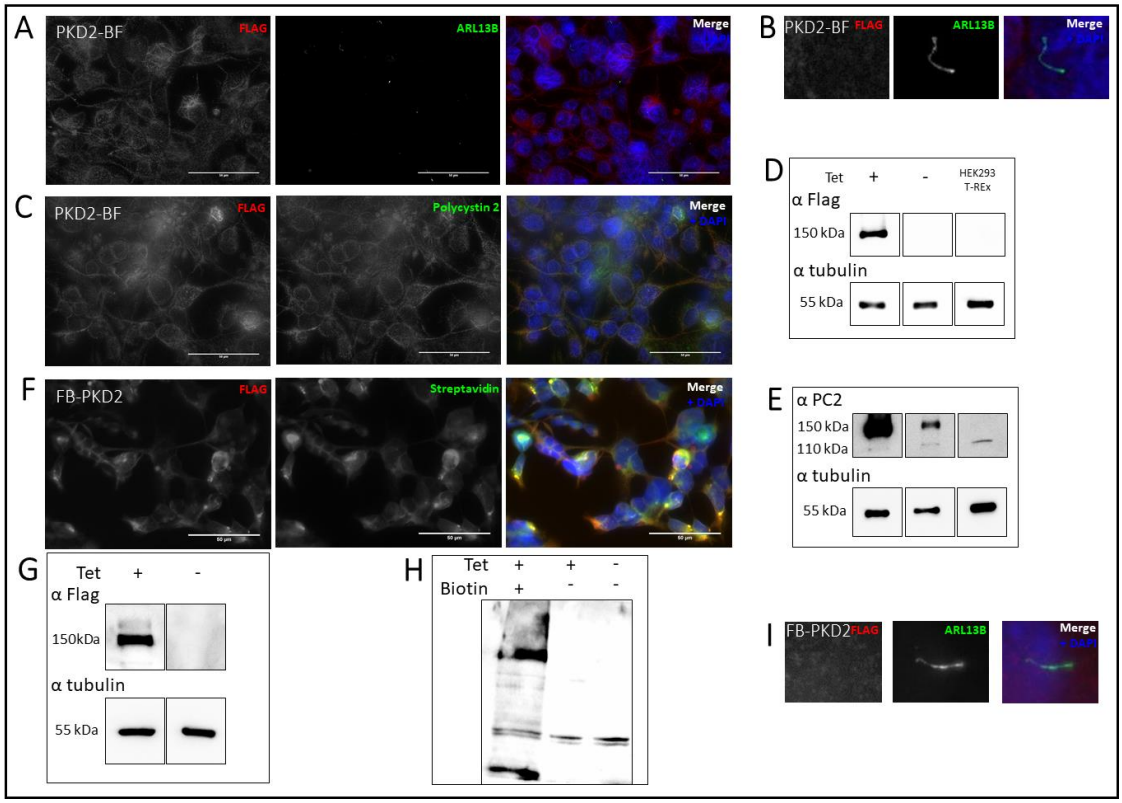

Figure 12. PKD2 BioID Construct Validation. (BF: BirAFLAG, FB: FLAGBirA) ***A-C****: Stably expressing PKD2-BirA in HEK 293 T-REx cells were subjected to IF staining to visualize cellular localization of PKD2 using anti-FLAG and anti-PC2, to confirm biotinylation using a Streptavidin probe (data not shown) and to investigate co-localization with ciliary marker ARL13B using anti-ARL13B.* ***D-E****: Western blot validation of PKD2-BirA fusion protein expression using anti-FLAG and anti-PC2. 110 kDa shows endogenous PC2 in the cell lysis.* ***F & I****: Stably expressing BirA-PKD2 in HEK 293 T-REx cells were subjected to IF staining to visualize cellular localization of PKD2 using anti-FLAG, to confirm biotinylation using a Streptavidin probe and to investigate co-localization with ciliary marker ARL13B using anti-ARL13B.* ***G-H****: Western blot validation of BirA-PKD2 fusion protein expression using anti-FLAG and Streptavidin (H) HRP.*

5.4 BioID and Mass Spectrometry of Stable PKD1 and PKD2 Cell Lines

All wild-type PKD1 and PKD2 BioID samples were processed and analyzed using Mass Spectrometry to identify candidate proximity interactors. The Mass Spectrometry was completed in collaboration with the Dr. Brian Raught Lab. Each cell line had two biological and two technical replications, as well as a non-ciliated and ciliated sample. Biotin and tetracycline were introduced 24hrs before processing and ciliated sample cells were starved 48hrs before processing to induce ciliation. We validated expression level by looking at BirA spectral counts (Table 1). The spectral count represents the amount of times the prey was biotinylated. Our data show consistent BirA expression, which allows us

to make comparisons between gain and loss of preys. However, the ciliated CD16.7-BirA control had significantly fewer BirA spectral counts (Table 1). This could have been due to cell death during the BioID processing. Because of this, I have normalized the ciliated CD16.7-BirA data based off the top 200 CD16.7-BirA preys. This gave me a spectral factor of ~3.9 and data was normalized as per the spectral factor. Each BioID sample had two technical replicates. The correlation between each replicate was compared and found to be similar (Figure 13).

Table 1. BirA peptide count between technical replicates.

Sample Name	BirA Peptide Count Technical Replicate 1	BirA Peptide Count Technical Replicate 1
BirA-PKD2	2980	2445
Ciliated BirA-PKD2	1987	1863
PKD2-BirA	2399	2220
Ciliated PKD2-BirA	1445	1260
CD16.7-PKD1-BirA	755	679
Ciliated CD16.7-PKD1-BirA	1198	983
CD16.7-BirA	1361	1211
Ciliated CD16.7-BirA	174	144

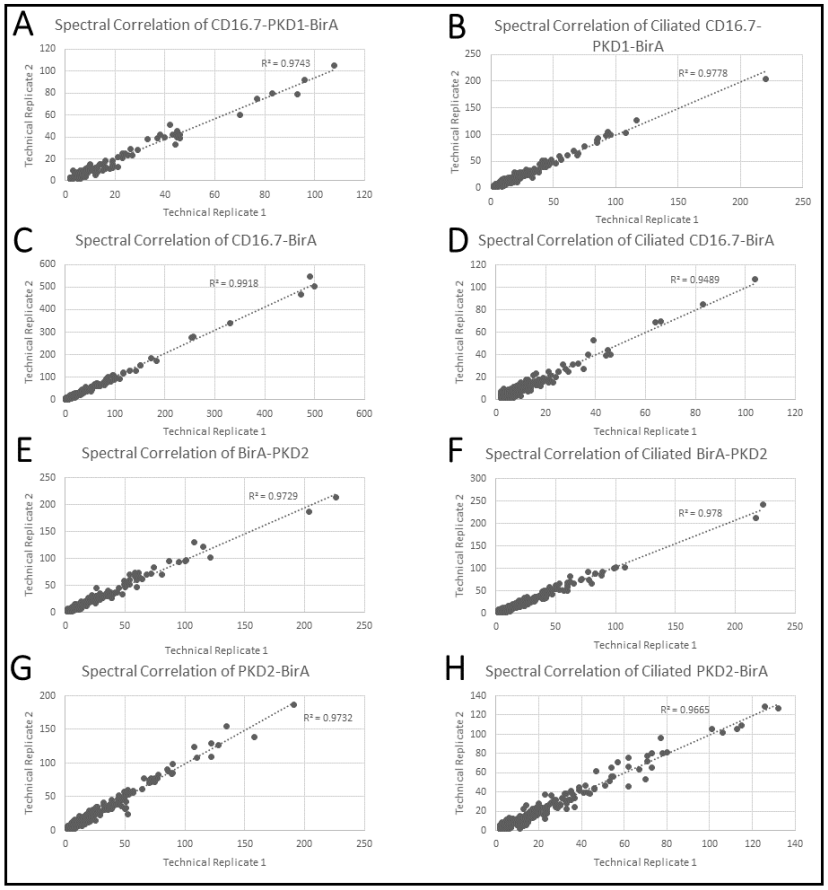

Figure 13. Correlation Analysis for PKD BioID samples. All preys were compared to show the consistency among replicates. X and Y axis represent spectral count. ***A****: n=156.* ***B****: n=271.* ***C****: n=602.* ***D****: n=325.* ***E****: n=322.* ***F****: n=384.* ***G****: n=411.* ***H****: n=343.*

5.4.1 Generation of Interactomes for Stable CD16.7-PKD1-BirA HEK293 T-REx Cell Line

BioID was completed for each sample which included a ciliated and non-ciliated sample. A Significance Analysis of the INTeractome (SAINT) was used to assign high confidence interaction scores to the interactome (Supp. Data 1). A SAINT score of ≥0.9 was applied to the protein-protein interaction (PPI) data as it corresponds to a false discovery rate (FDR) of 1% (Choi et al., 2011). The CD16.7-PKD1-BirA interactome was generated in the HEK293 T-REx cell line with a ciliated sample and non-ciliated sample. The CD16.7-PKD1-BirA ciliated sample resulted in 271 high confidence interactors and the CD16.7-PKD1-BirA non-ciliated sample resulted in 156 high confidence interactors (Table 2, Figure 14, Figure 21). Among these two samples, 124 high confidence interactors were shared. Of the entire CD16.7-PKD1-BirA PPI, including both ciliated and non-ciliated samples, 287 were cilia-associated genes

when compared to the Cilia Database (Table 2, Figure 14; Arnaiz et al., 2014). Gene Ontology (GO) was completed using GO-Panther (Figure 15A & 15B; Mi et al., 2019) where it was determined numerous membrane trafficking and transporter activity genes were associated with ciliated CD16.7-PKD1-BirA.

Table 2. Representation of High-Confidence Proximity Interactors were detected in each BioID sample.

Sample Name	High-Confidence Proximity Interactors		
	Non-Ciliated	Ciliated	Shared
BirA-PKD2	322	384	260
PKD2-BirA	411	343	268
CD16.7-PKD1-BirA	156	271	124

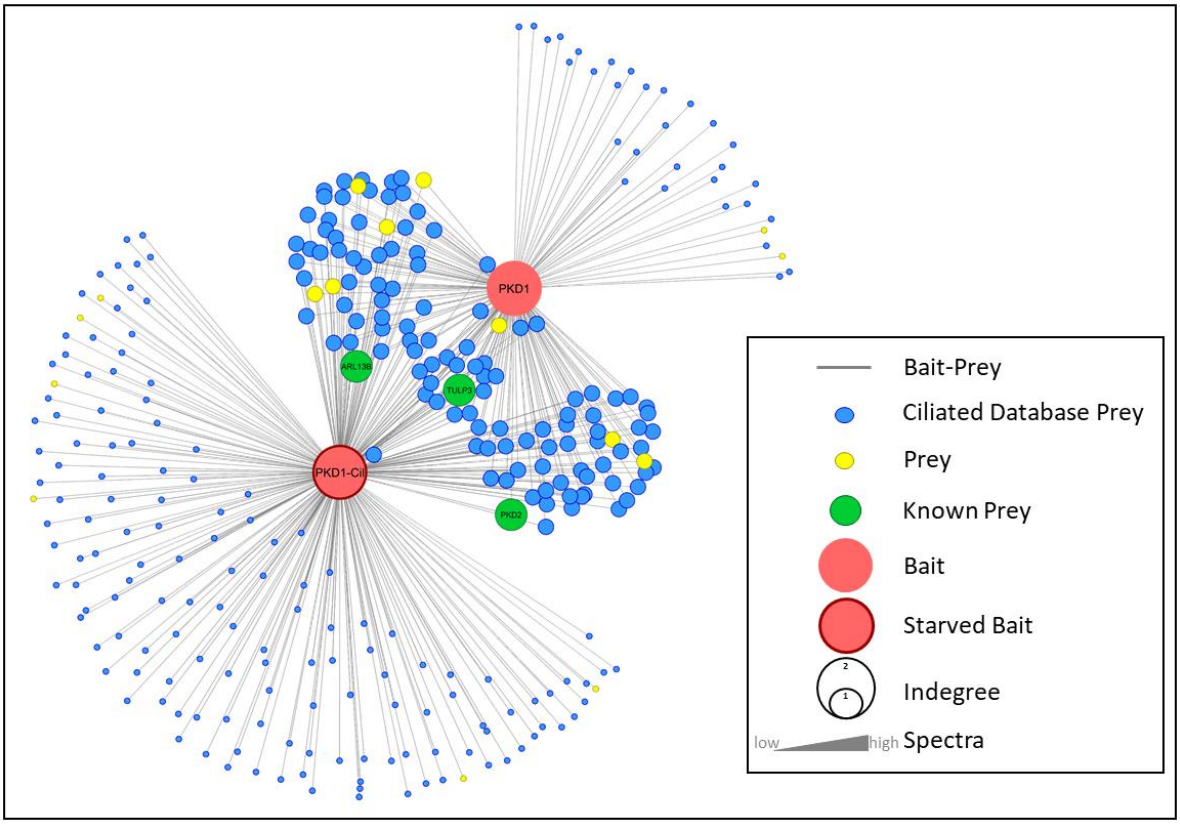

Figure 14. CD16.7-PKD1-BirA Interactome. Map created using Cytoscape representing a spring loaded edge-weighted network of the CD16.7-PKD1-BirA BioID data. Bait and preys are shown as circles in the legend above. The interactome contains an enrichment of cilia-associated genes as per the Cilia Database (see text).

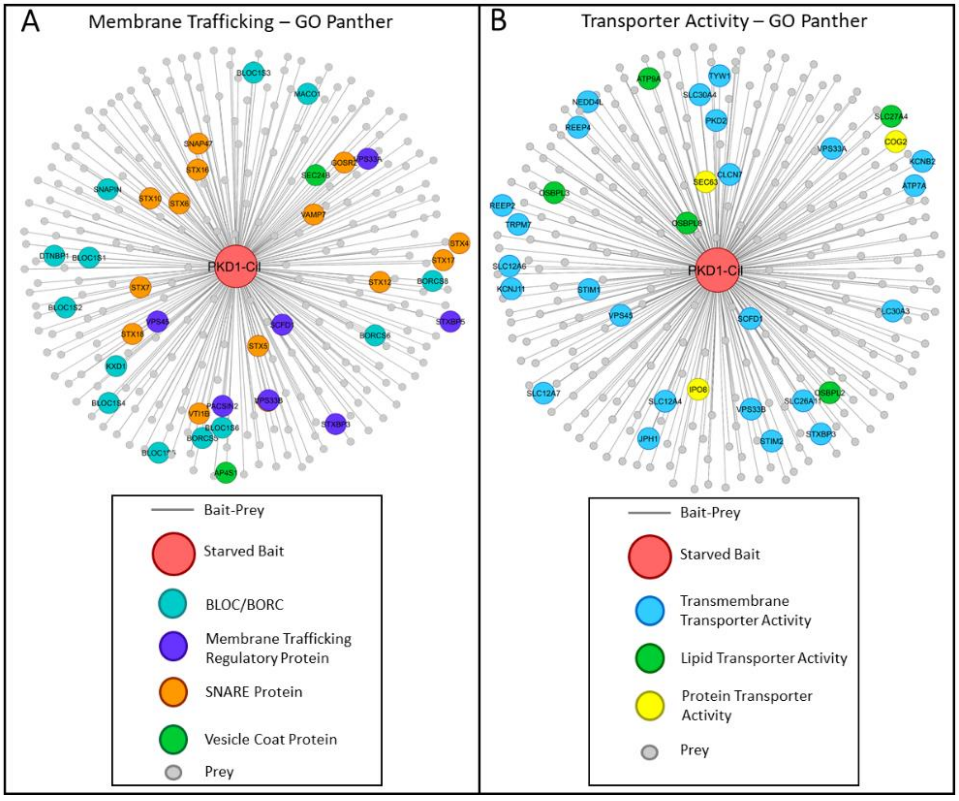

Figure 15. Gene Ontology of CD16.7-PKD1-BirA Ciliated BioID Sample. Panels A and B are colour-coded to show enrichment of functional categories.

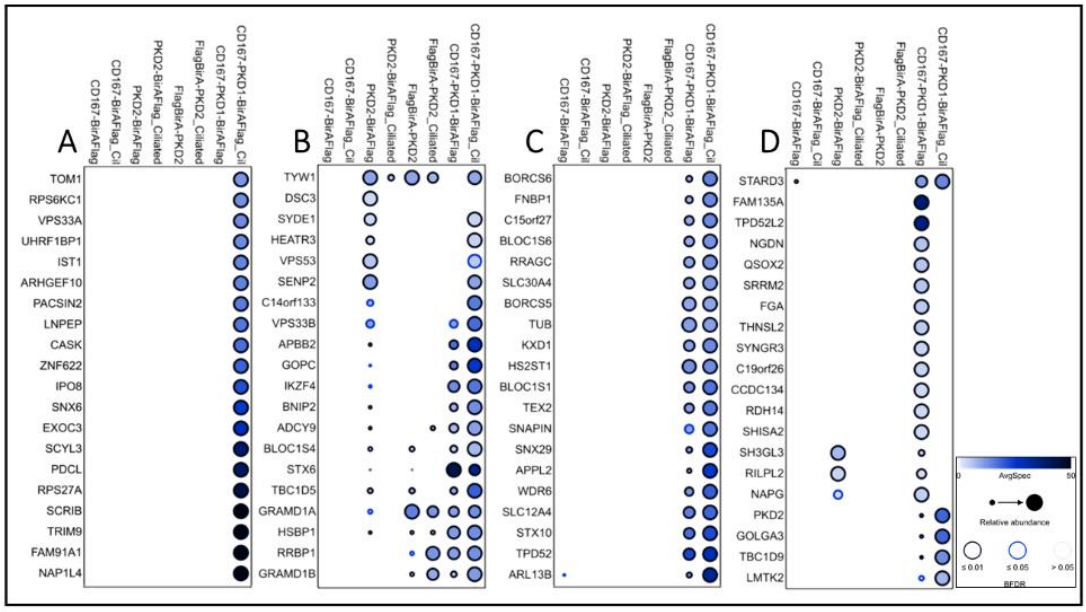

Figure 16. Dot Plot Showing Examples of Various Trends in the BioID Samples. The legend is in the bottom right corner. A: There are several preys that appear to only interact with the cilia induced PKD1 CTT. B: There is a wide range of preys that interact with some but not all BioID samples. C: There are several preys that appear in both PKD1 samples, but enriched in the ciliated sample. D: There are some preys that appear to only interact with PKD1 CTT when the cells are not ciliated. Additionally, there are some interactions that occur between PKD2 CTT and

PKD1 CTT (Such as SH3GL3, RILPL2 and NAPG).

5.4.2 Generation of Interactomes for Stable PKD2-BirA and BirA-PKD2 HEK293 T-REx Cell Lines

Like the CD16.7-PKD1-BirA interactome, the PKD2-BirA and BirA-PKD2 interactomes were generated in the HEK293 T-REx cell line with a ciliated sample and non-ciliated sample (Supp. Data 1). A SAINT score of ≥0.9 was applied to the PPI data as it corresponds to a false discovery rate (FDR) of 1% (Choi et al., 2011). The PKD2-BirA ciliated sample resulted in 343 high confidence interactors and the PKD2-BirA non-ciliated sample resulted in 411 high confidence interactors (Table 2, Figure 7, Figure 21). Among these two samples, 268 high confidence interactors were shared. The BirA-PKD2 ciliated sample resulted in 384 high confidence interactors and the BirA-PKD2 non-ciliated sample resulted in 322 high confidence interactors (Table 2, Figure 17, Figure 21). Among these two samples, 260 high confidence interactors were shared. The N- and C-terminal PKD2 vectors, including both ciliated and non-ciliated samples, share 180 high-confidence interactors (Figure 17). Gene Ontology (GO) was completed using GO-Panther (Mi et al., 2019) where it showed an enrichment of ER-associated genes and much fewer membrane-associated genes (data not shown). This data is consistent with immunofluorescent localization of PC2 and is thus not a good representation of PC2 ciliary function or trafficking. However, PC2 does function at the ER, so the discovered PPI should not be ignored. However, the purpose of this research is to study ciliary PC1 and PC2, thus the remainder of the report will focus on the CD16.7-PKD1-BirA interactome.

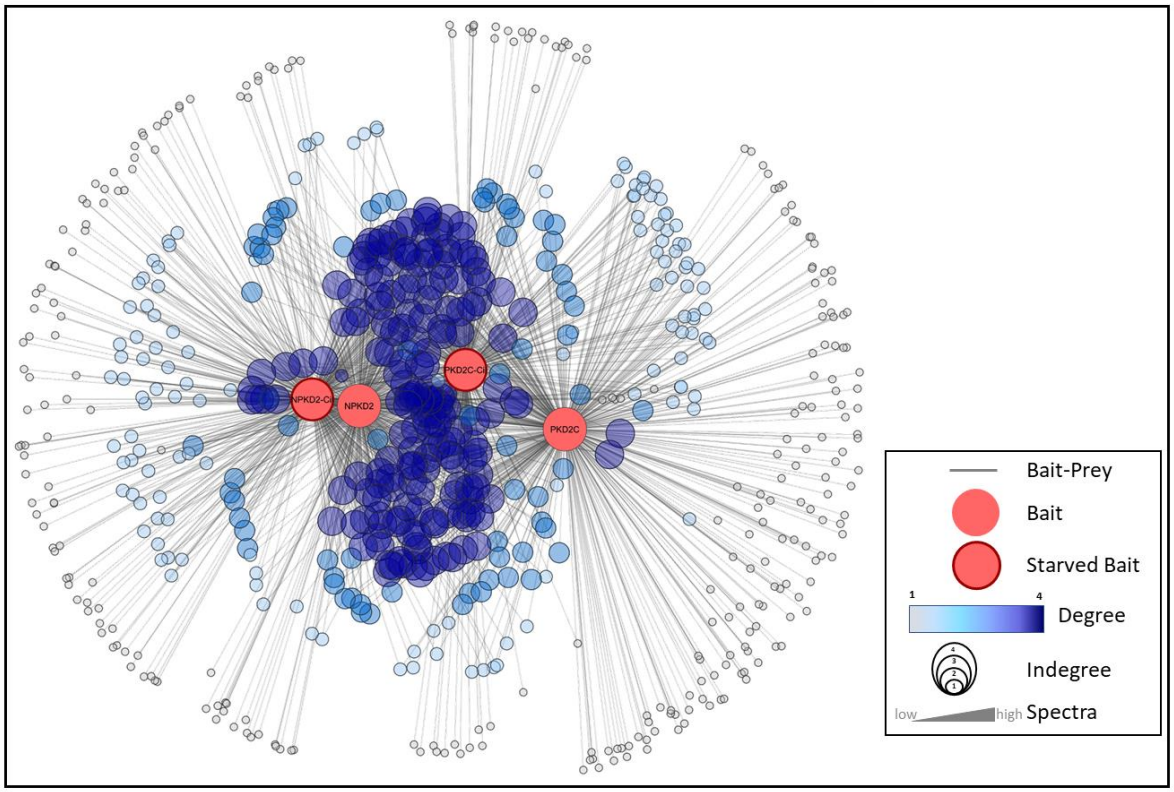

Figure 17. PKD2 BioID Interactome. Map created using Cytoscape representing a spring loaded edge-weighted network of the BirA-PKD2 and PKD2-BirA BioID data. Bait and preys are shown as circles in the legend above.

5.4.3 Comparison of Ciliated Interactome to Non-Ciliated Interactome

The ciliated CD16.7-PKD1-BirA interactome data shows more PPIs than the non-ciliated sample (Table 2, Figure 14, Figure 21). As well, among the 124 ciliated and non-ciliated shared interactions, 65 are enriched 1.5-fold in the ciliated sample (Figure 18). There are 147 unique interactions in the ciliated sample, and 32 unique interactions in the non-ciliated sample (Figure 14). In contrast to the CD16.7-PKD1-BirA immunofluorescence localization, it is evident that the chimeric PC1 CTT fusion protein is trafficking to cilia. For example, two well-characterized ciliary proteins, TULP3 and ARL13B appears in proximity to the PC1 CTT in both samples but is enriched in the ciliated sample ~3-fold (Figure 20B & C). This shows that PC1 CTT is translocating to cilia, confirming that the CD16.7-PKD1-BirA fusion construct is an adequate representation of ciliary PC1 CTT.

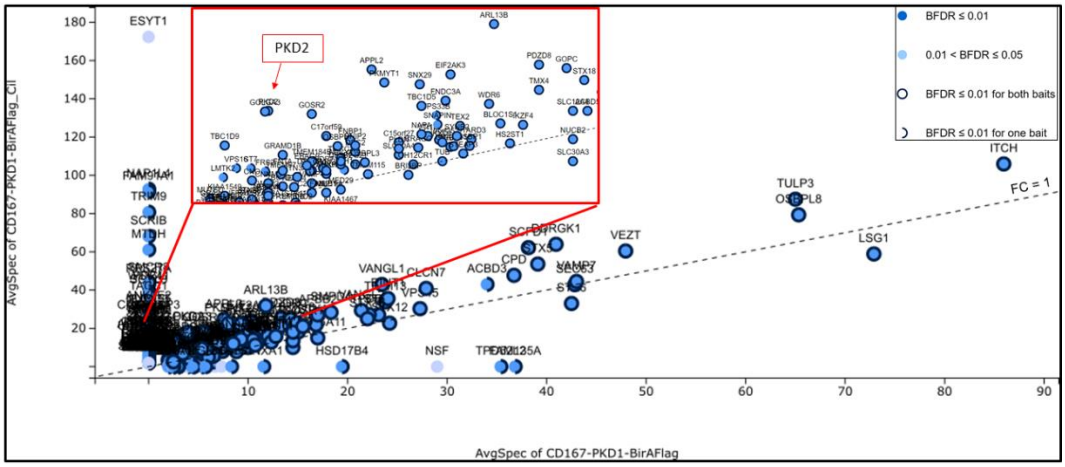

Figure 18. Scatter Plot created from https://prohits-viz.lunenfeld.ca/ of CD16.7-PKD1-BirA interactome. The preys were filtered from the CD16.7-PKD1 control. A zoomed in representation of the clustered data is shown in the red box.

5.5 Noteworthy Candidate Genes

There are currently only a few known PPI associated with PC1. This makes it difficult to confirm known interactors as a "proof of concept". Notably, PKD2 was identified in both CD16.7-PKD1-BirA samples and enriched 4.5-fold in the ciliated interactome (Figure 16; Figure 18A). Moreover, there are some known PC2 interactions that appear in the PC1 interactome. Such genes that have been proposed to be required for PC2 ciliary trafficking: TULP3 (Figure 14, Figure 20C; Badgandi et al., 2017; Hwang et al., 2019; Legué et al., 2019) and BLOC1S6 (Figure 20I; Monis et al., 2017). This could suggest that PC1 and PC2 traffic to cilia together, potentially as a complex. Unfortunately, there are no other TULP3 interactors or Tubby-Family proteins in the CD16.7-PKD1-BirA PPI data, so there is no indication if other proteins assist in the trafficking. BLOC1S6 is a subunit of the complex Biogenesis of Lysosome-related Organelles Complex-1 (BLOC-1). Strikingly, the CD16.7-PKD1-BirA exhibits all eight subunits of the BLOC-1 complex and most of the BLOC-One Related Complex (BORC) (Figure 15A, Figure 19; Figure 20D-O). A recent finding suggests that BLOC-1 is involved in an endosomal pathway whereby proteins traverse the recycling endosome on the way to the cilium (Monis et al., 2017). In addition, BLOC-1 and BORC are interacting partners (Langemeyer et al., 2015). This suggests that PC1 CTT likely traffics through the recycling endosome pathway, a new trafficking pathway that could be disrupted in ADPKD.

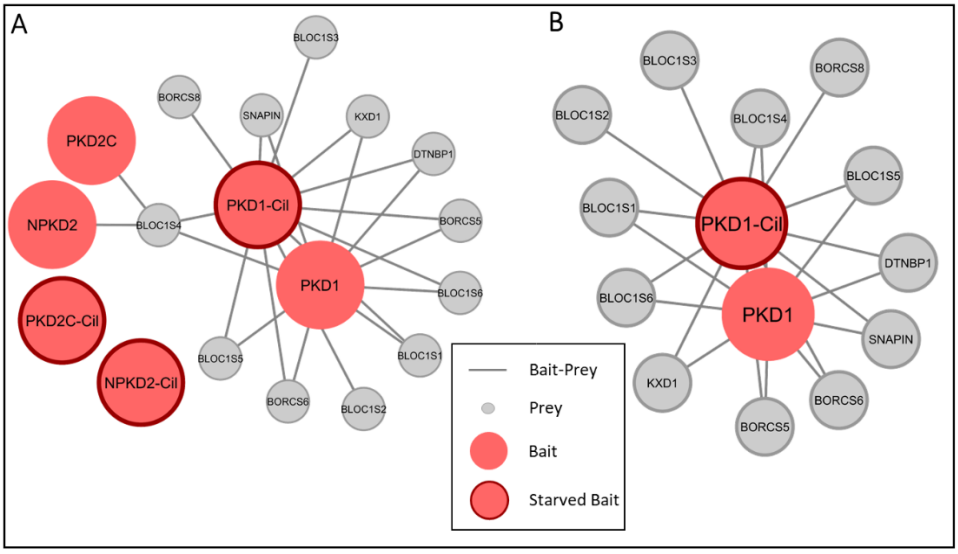

Figure 19. Cytoscape Map of BLOC-1 and BORC Complex Subunits. A: All PKD samples were visualized to show the enrichment of BLOC-1/BORC subunits. B: Visualization of only CD16.7-PKD1-BirA BLOC-1/BORC proximity interactors.

Interesting candidate interactors were identified through analysis of the PPI data. The data was filtered by average spectral count (AvgSpec), uniqueness to other baits, enrichment in ciliated samples, specificity to bait by Human Cell Map (Go et al., (in preparation)), Gene Ontology (Mi et al., 2019), localization based on protein atlas (Uhlen et al., 2017), if up or down regulated in cystic tissue experiments (Supp. Table 1) and if it was a ciliary-associated gene based on Cilia Database (Arnaiz et al., 2014). From this analysis, we were able to identify the following interesting candidate interactors: BLOC1S2, SYNE2, SEC63 and OSBPL8 (Figure 20).

BLOC1S2, Biogenesis of Lysosomal Organelles Complex 1 Subunit 2, is a member of the BLOC-1 complex as mentioned earlier in this section. We think this is an interesting candidate to explore as it appears exclusively in the CD16.7-PKD1-BirA ciliated interactome and has previously been shown to localize to the centrosome (Figure 20E; Wang et al., 2004). We also think BLOC1S2 would be a good starting point to understanding PC1's role in the BLOC-1 and BORC complex. Ultimately, it would be necessary to explore all BLOC-1 and BORC subunits.

SYNE2, Nesprin-2, is another gene of interest as it has been demonstrated to be involved in early stages of ciliogenesis (Figure 20P; Falk et al., 2018). It is important in centrosomal migrating during early ciliogenesis as a CRISPR/Cas9-mediated knock out of SYNE2 lead to mislocalization of Pericentrin, a centrosomal protein, and ciliogenesis defects were observed (Falk et al., 2018). Additionally, SYNE2 interacts with SUN1 and SUN2, both of which we observe in the BioID PPI data. Their interaction was shown to connect the centrosome to the nucleus in mice during neuronal migration (Zhang et al., 2009; Yu et al., 2011).

SEC63 when mutated causes Polycystic Liver Disease (PLD) (Figure 20Q). PLD patients have cystic livers, but also mild cystic kidneys, whereas PKD patients have cystic kidneys but also mild cystic livers. Patients experience more aggressive cyst formation on the diseased organ (Chebib et al., 2018). The disease phenotypes in PKD and PLD could suggest that SEC63 and PKD1 and/or PKD2 function in the same pathway. ADPKD mouse mutants were used to show that loss of SEC63 leads to more aggressive cyst formation. As well, loss of SEC63 blocks PC1 trafficking to primary cilia and reduced PC1 and PC2 expression (Fedeles et al., 2011; Fedeles et al., 2015). Understanding the relationship between PKD and PLD-causing genes could provide insight to cystogenesis.

ADPKD patients with a mutation in PKD1 were found to have abnormal hypermethylation on the diseased gene. OSBPL8, Oxysterol Binding Protein Like 8, was found to also be hypermethylated in a genome-wide methylation profiling of ADPKD (Figure 20R; Woo et al., 2004). Understanding the regulated genes associated with renal cyst development could lead to further epigenetic therapies for ADPKD patients. It has been demonstrated that OSBPL8 is a lipid transporter that could play a role in membrane trafficking mediated by vesicular and non-vesicular pathways (Zhou et al., 2011; Chung et al., 2015). Nevertheless, the relationship between OSBPL8 and either of the polycystins in completely unknown, though it has high spectral counts in all BioID samples (Figure 20R).

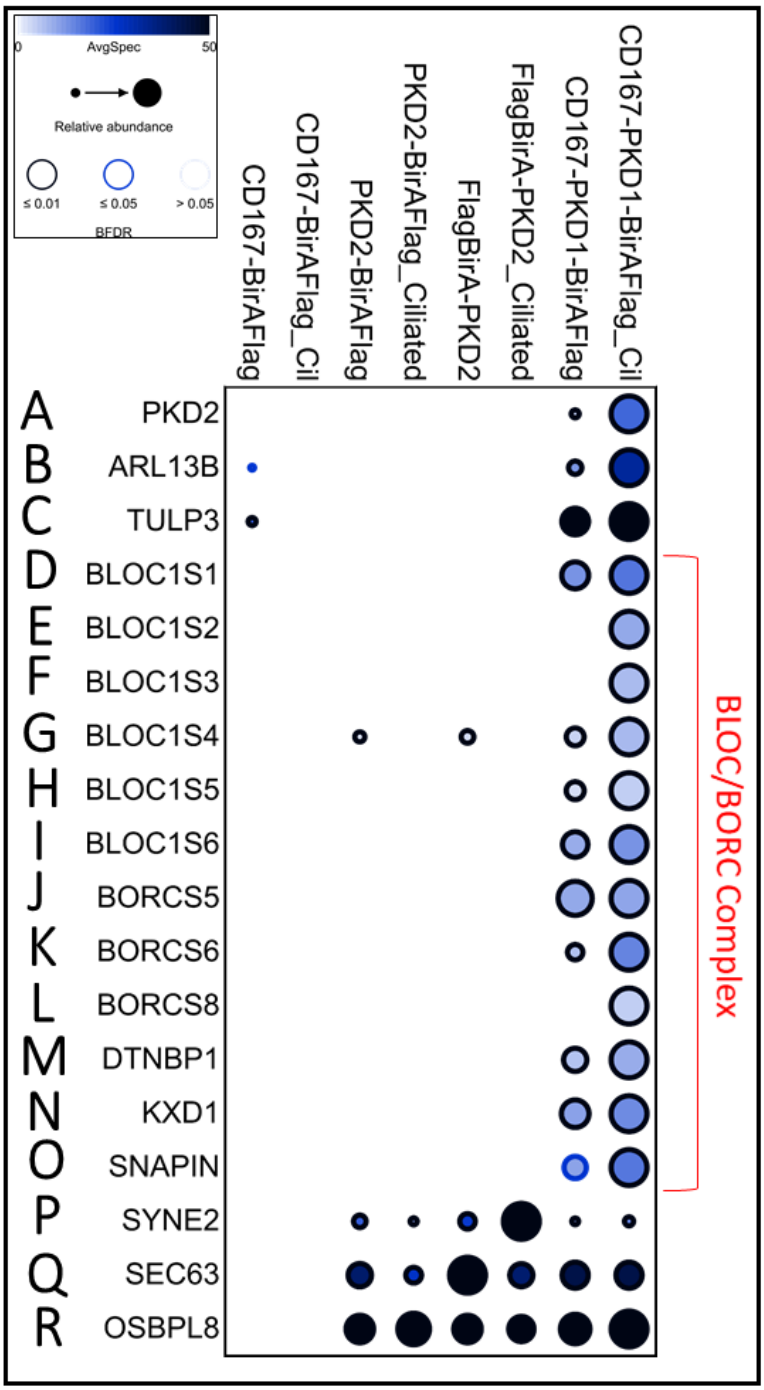

Figure 20. Dot Plot Created From https://prohits-viz.lunenfeld.ca/ Showing Enrichment of Spectral Count in all PKD BioID samples and controls. A-C: Proof of concept interactions. D-O: BLOC-1 and BORC complex subunits. P-R: Interesting candidate preys (see text).

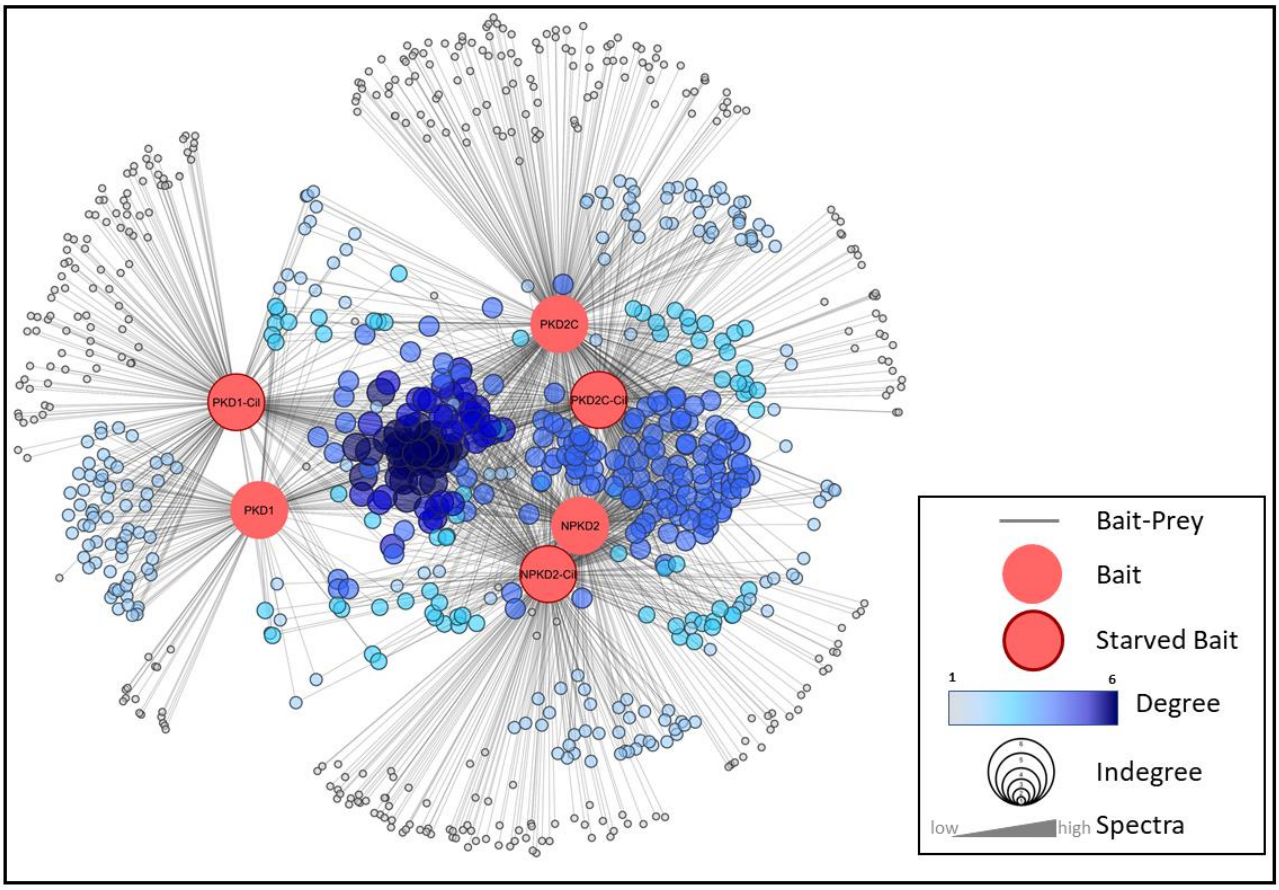

Figure 21. PKD BioID Interactome. Map created using Cytoscape representing a spring loaded edge-weighted network of all BioID data. Bait and preys are shown as circles in the legend above.

6.0 Discussion

Functional PC1 and PC2 appear to play an essential role in maintaining healthy kidneys. Mutations in these genes impact their ciliary localization and lead to cystic kidneys. We hypothesized that, as part of its function and traffic, PC1 and PC2 must interact with unknown targets. These targets could be critical in our understanding of ADPKD and polycystin function, however, remain largely unknown. Using BioID, a proximity-labeling technique, numerous putative PC1 binding proteins were identified that likely mediate the effects of polycystin on ciliary trafficking and ciliogensis.

6.1 BioID and AP-MS to Identify New Interacting Proteins

PPI techniques such as Co-Immunoprecipitation and Yeast-2-Hybrid are well suited for detection of interactions that are strong and direct. However, these techniques have limitations, including only being able to test if known proteins interactions are direct or strong using a specific protein-antibody reaction. BioID overcomes these limitations by screening for strong and direct interactions, as well as weak or transient interactions. This technique can identify additional protein interactions and even identify novel interactions that would otherwise be missed in other PPI techniques. This research used BioID to biotinylate endogenous proteins along the C-terminus of PC1, and both the N- and C-termini of PC2. The promiscuous biotin ligase (BirA*) was fused onto the polycystin termini and facilitated the capture of any transient, indirect and direction protein-protein interactions.

6.2 The PC1 Carboxy Terminal Interacts with BLOC-1 and BORC Families

Cells distribute their lysosomes to facilitate interactions with phagosomes and endosomes during protein turnover (Korolchuk et al., 2011). Lysosomal positioning within the cytoplasm is critical for many lysosomal functions. Two protein complexes, Biogenesis of Lysosome-Related Organelles Complex-1 (BLOC-1) and BLOC-One-Related Complex (BORC) forms a multi-subunit complex that appears to regulate lysosome positioning (Ping et al., 2015). The BLOC-1 complex is composed of eight subunits, found on tubular endosomes and thought to be required for the biogenesis of lysosome-

related organelles. The protein has an unknown function but interacts in vitro with four of the BORC subunits. BLOC-1 subunit, BLOC1S2, was discovered to localize not only to the cytoplasm, but also the centrosome, however its role at the centrosome, cilia and PKD remains unknown (Wang et al., 2004). The BORC complex is also composed of eight subunits, three of which are shared with BLOC-1 (Figure 22). Interestingly, the PC1 CTT interacts with all BLOC-1 subunits, and seven of the eight BORC subunits. The relationship between PC1 and BLOC/BORC has not been discussed in literature.

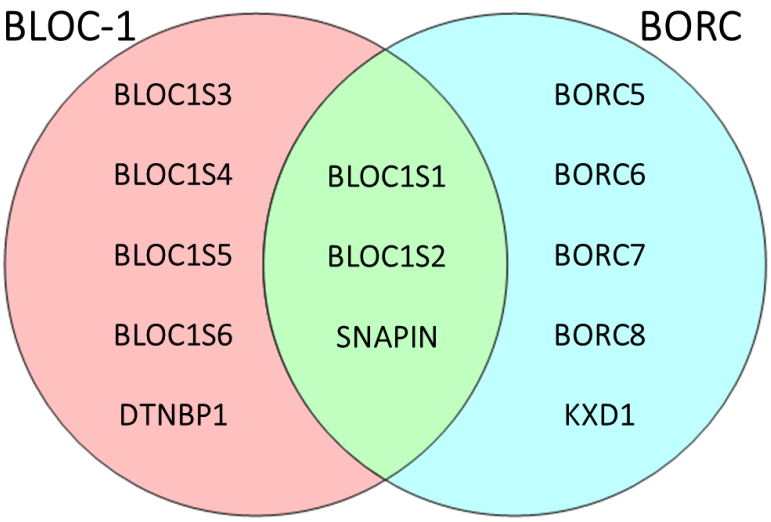

Figure 22. Composition of BLOC-1 and BORC subunits.

It is important that translated proteins are delivered to their specific cellular location, and for this to occur, the protein is transferred through a series of membrane structures. Membrane proteins fold in the ER, are generally sent to the Golgi apparatus where they are sorted, modified and packaged into vesicles for delivery to target membranes. The vesicular delivery of membrane fusion proceeds through various steps involving a cascade of Rab GTPases and its effectors, tethering complexes such as the exocyst complex, and SNAREs (soluble N-ethylmaleimide-sensitive factor attachment protein receptor). It remains unknown how PC1 or PC2 are sorted, modified and packaged in the Golgi apparatus, as well as how they are delivered and tethered to the target membrane. The BioID data reveals that the PC1 CTT interacts with some vesicular transport complexes known to be involved in the

endosome recycling pathway transport, which could reveal its ciliary trafficking mechanism (Figure 23; Table 3).

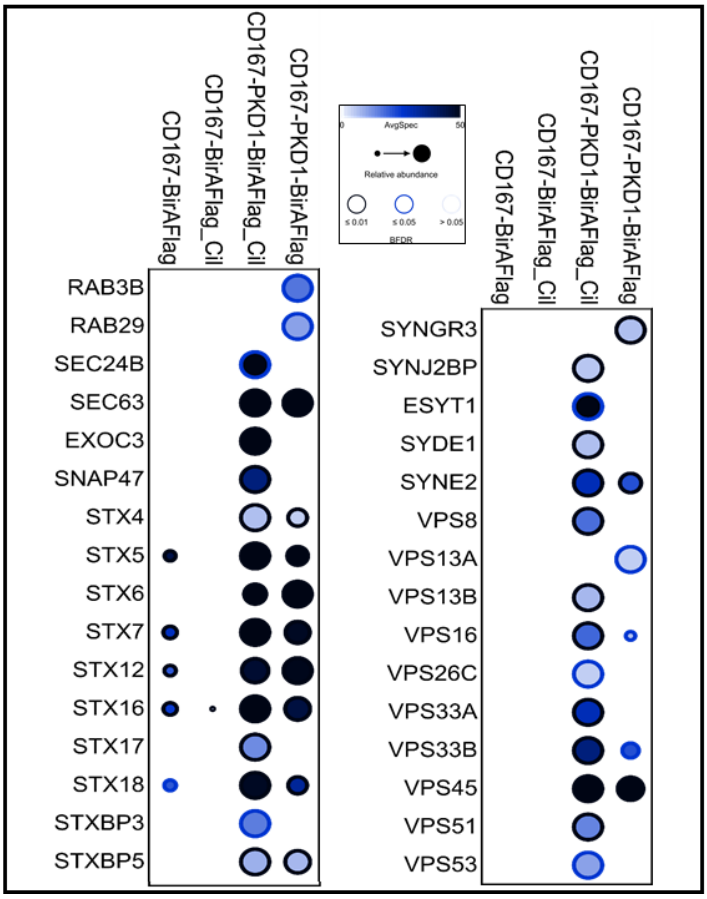

Figure 23. Dot Plot Created From https://prohits-viz.lunenfeld.ca/ Showing Enrichment of Spectral Count in some Vesicular Trafficking Associated Genes.

Table 3. Summary of candidate BioID genes interacting with PC1 CTT with implicated membrane trafficking roles.

Gene	Complex	Function	Reference
RAB3B	Member RAS Oncogene Family	Likely to be involved in vesicular trafficking, GTP binding and GDP binding. A component of Weibel-Palade body exocytosis.	Bierings et al., 2012 Karniguia et al., 1993
RAB29		Plays a role in the retrograde trafficking pathway for recycling proteins between lysosomes and the Golgi apparatus.	Wang et al., 2014
SEC24B	COPII Coat Complex Component	The encoded protein is thought to be a cargo-binding component of the COPII vesicle and is thought to be involved in the transport of secretory proteins from the ER to the Golgi apparatus.	Mancias & Goldberg, 2008
SEC63	Protein Translocation	It is speculated that the Sec61-Sec62-Sec63 complex may perform post-translational protein translocation into the ER.	Lang et al., 2012

	Regulator, SEC61-SEC62-SEC63		
EXOC3	Exocyst Complex	Involved in the docking of exocytic vesicles with fusion sites on the PM.	Ganesan et al., 2020
SNAP47	Synaptosome	Regulates behavior of the fusion pore between the vesicle and PM, temporarily arresting the pore in an open state.	Urbina et al., 2020
STX4	Syntaxin	PM t-SNARE that mediates docking of transport vesicles. Together with STXB3 and VAMP2, may also play a role in docking/fusion of intracellular GLUT4-containing vesicles.	Veale et al., 2011
STX5		This gene encodes a member of the syntaxin or t-SNARE family. These proteins are found on cell membranes and serve as the targets for v-SNAREs, permitting specific synaptic vesicle docking and fusion.	Wagner et al., 2013
STX6		Is required for the fusion between vacuoles and recycling endosomes to promote clearance by autophagy.	Nozawa et al., 2017
STX7		Binds alpha-SNAP and pays a role in the ordered fusion of endosomes and lysosomes with the phagosome.	Achuthan et al., 2008
STX12		SNARE that acts to regulate protein transport between late endosomes and the TGN, mediating vesicle fusion.	Tang et al., 1998
STX16		SNARE involved in vesicular transport from the late endosomes to the TGN.	Dulubova et al., 2002
STX17		SNARE of the autophagosome involved in autophagy through the direct control of autophagosome membrane fusion with the lysosome membrane. May also play a role in the early secretory pathway where it may maintain the architecture of the ER-Golgi intermediate compartment (ERGIC) and Golgi and/or regulate transport between the endoplasmic reticulum, the ERGIC and the Golgi.	Muppirala et al., 2011
STX18		May be involved in targeting and fusion of Golgi-derived retrograde transport vesicles with the ER.	Hatsuzawa et al., 2000
STXBP3	Syntaxin Binding	Together with STX4 and VAMP2, may play a role in insulin-dependent movement docking/fusion of vesicles with the cell surface in adipocytes.	Hodgkinson et al., 2005
STXBP5		Plays a regulatory role in Ca^{2+}-dependent exocytosis. Inhibits membrane fusion between transport vesicles and the PM. May modulate the assembly of t-SNARE complexes between transport vesicles and the PM.	Zhu et al., 2014
ESYT1	Extended Synaptotagmin	Helps tether the ER to the cell membrane and promotes the formation of appositions between the ER and the cell membrane.	Sclip et al., 2016
SYDE1	Rho GTPase-activating protein	It regulates cytoskeletal remodeling by controlling the activity of some Rho GTPases.	Lo et al., 2017
SYNE2	Nuclear Envelope Protein	Tethers the nucleus to the cytoskeleton and aids in the maintenance of the structural integrity of the nucleus.	Yu et al., 2011
SYNGR3	Synaptogyrin	Unclear	N/A
SYNJ2BP	Synaptojanin	SYNJ2BP plays a variety of cellular functions by combining with different proteins, including binding proteins for endocytosis localization, cycling and degradation. In addition, SYNJ2BP may also regulate the PI3K signal pathway through the autophagy-lysosome-associated degradation of	Wang et al., 2017

		PTEN, suggesting that SYNJ2BP might be closely associated with lysosome membrane proteins.	
VPS8	Vacuole Protein Sorting	Plays a role in vesicle-mediated protein trafficking of the endocytic membrane transport pathway. Believed to act as a component of the putative CORVET endosomal tethering complexes.	Perini et al., 2014
VPS13A		May play a role in the control of protein cycling through the TGN to early and late endosomes, lysosomes and PM.	Kumar et al., 2018
VPS13B		May be involved in protein sorting in post Golgi membrane traffic.	Ionita-Laza et al., 2014
VPS16		Plays a role in vesicle-mediated protein trafficking to lysosomal compartments including the endocytic membrane transport and autophagic pathways. Believed to act as a core component of the putative HOPS and CORVET endosomal tethering complexes and via binding SNAREs and SNARE complexes to mediate tethering and docking events during SNARE-mediated membrane fusion.	Wartosch et al., 2015
VPS26C		In the endosomes, drives the retriever and recycling of NxxY-motif-containing cargo proteins by coupling to SNX17, a cargo essential for the homeostatic maintenance of numerous cell surface proteins associated with processes that include cell migration/adhesion, nutrient supply and signaling.	McNally et al., 2017
VPS33A		A tethering protein and a core subunit of the homotypic fusion and protein sorting (HOPS) complex.	Solinger et al., 2013
VPS33B		May play a role in vesicle-mediated protein trafficking to lysosomal compartments and in membrane docking/fusion reactions of late endosomes/lysosomes. Proposed to be involved in endosomal maturation implicating VIPAS39.	Bach et al., 2008 Cullinane et al., 2013
VPS45		May play a role in vesicle-mediated protein trafficking from the Golgi stack through the TGN.	Dulubova et al., 2002
VPS51		A component of the Golgi-associated retrograde protein complex which acts as a tethering factor for carriers in retrograde transport from the early and late endosomes to the TGN.	Reggiori et al., 2003
VPS53		Acts as component of the GARP complex that is involved in retrograde transport from early and late endosomes to TGN.	Hausman-Kedem et al., 2019

This research reveals a new trafficking mechanism for PC1 that could be regulated by BLOC-1 and BORC complexes. These complexes rely on an interconnected membrane system and recruitment factors on lysosomes or endosomes, which have yet to be determined for BORC or BLOC-1 (John Peter et al., 2013). The characterization of the BORC subunits (Figure 22) provides information to the complexes involved in trafficking, transport, and signaling. Similar complexes are the HOPS and CORVET tethering complexes including VPS11, 16, 18, and 33; many of which are found to be proximity interactors with PC1 CTT (Figure 23; Table 3). To date, there has been no link from the BLOC-1 and BORC

complexes to PC1. This research suggests that PC1 could selectively traffic from endosomes to cilia. Subsequently, it was shown that BLOC-1 is necessary for PC2 selective trafficking from endosomes to cilia, however its relationship with PC1 was not explored (Monis et al., 2017). If PC1 requires BLOC-1 for ciliary localization, it would suggest that PC1 and PC2 traffic together.

6.3 PC1 and PC2 Proximally Interact with Nesprin-2

Interkinetic nuclear migration (INM) is the mechanism in which the nucleus migrates throughout the cell during cycling (Kulikova et al., 2011). The KASH-domain protein Neprin-2 (SYNE2) was recently shown to play a critical role during INM in mice. SYNE2 forms a complex with SUN1 and SUN2 to mediate coupling of the centrosome to the nucleus during INM (Zhang et al., 2009). SYNE2 was identified as a PC1 and PC2 proximity interacting partner (Figure 24). Interestingly, SUN1 and SUN2 were also identified as proximity interactors. The relationship between these candidate genes and the polycystins in INM remains unclear.

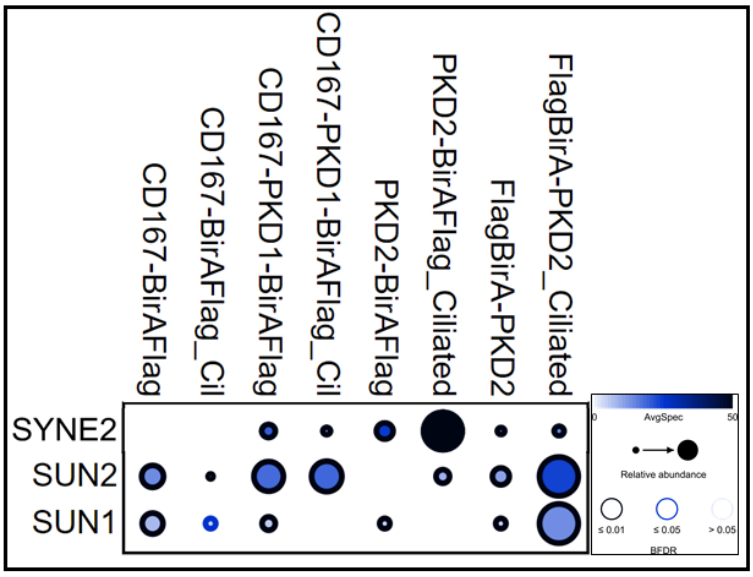

Figure 24. Dot Plot Created From https://prohits-viz.lunenfeld.ca/ Showing Enrichment of Spectral Count in Interkinetic Nuclear Migration.

SYNE2 is an outer nuclear membrane protein with multiple isoforms. It was recently shown to be important for centrosomal migration during early stages of ciliogenesis. Lack of SYNE2 led to mislocalization and overexpression of a well known centriolar protein, pericentrin (PCNT). PCNT was mislocalized in the Golgi membranes, suggesting that SYNE2 may form complexes with centriolar proteins, such as PCNT, or other proteins important for ciliogenesis and outer segment formation during nuclear migration (Falk et al., 2018). PCNT was not shown to interact with the baits used in this research, however, several other ciliary genes involved in ciliogenesis were identified including ARL13B. It is unclear the role, if any, PC1 and PC2 play in ciliogenesis, however these interactions suggest an additional pathway that they polycystins may play a role in.

6.4 PC1 and PC2 Proximally Interact with SEC63

A common phenotype of ADPKD is mild cystic livers. Polycystic Liver Disease (PLD) is like ADPKD as it is an autosomal dominant disorder characterised by fluid filled cysts, except on the liver (Janssen et al., 2012). PLD is caused by a heterozygous germline mutation in PRKCSH and SEC63. Inexplicably, patients experience mild cystic kidneys as well. Like PKD, the relationship to cyst formation in PLD remains unknown. One of the PLD causing genes, SEC63 was identified as a PC1 and PC2 proximity interacting partner in this research. SEC63 is a component of the protein translocation machinery in the ER, along with SEC61 and SEC62. It plays an important role for membrane proteins in post-translational translocation and mutations likely diminish its function (Jung et al., 2019).

SEC63 knockout mice experience cysts on the liver and kidney due to reduced function of PC1 (Fedeles et al., 2011). Additionally, in PKD2 mice, the loss of SEC63 increases the aggression of cyst formation. These suggests that there is a relationship between the polycystins and SEC63 (Fedeles et al., 2015). Perhaps, SEC63 is essential for the ER topogenesis of membrane proteins associated with PKD such as PC1 or PC2. However, the other PLD-causing mutation, PRKCSH was not determined to be a

proximity interactor with the PC1 CTT bait, as there was equal biotinylation in the CD16.7 control, nor did it interact with the PC2 baits.

6.5 PC1 and PC2 Proximally Interact with Oxysterol Binding Protein Like 8

The Oxysterol binding protein (OSBP) family localizes mainly on the Golgi-membrane in a sterol-specific manner, regulating the trafficking lipids from the ER to the Golgi apparatus for sphinghomyelin systhesis (Perry et al., 2006). Sphinghomyelin is a member of the sphingolipid family that is a PM component participating in various signaling pathways. It is a class of PM lipids that can modulate the formation and function of cilia and membrane microdomains, receptor signaling activity, lysosomal function and cell recognition. A characteristic of ADPKD is a change in lipid metabolism leading to the accumulation of sphingolipids (Shayman et al., 2018). The accumulation of various sphingolipids appears to drive cyst formation and growth in ADPKD. Understanding the role that OSBPs and shingolipids play in cyst formation and growth could shed light on polycystin function.

This research demonstrates a relationship with one of the OSBP family members, OSBPL8, as a significant proximity interactor with both PC1 and PC2 (Figure 20R). The protein product of OSBPL8 is localized at the ER and plays an important role in regulating the cellular lipidome. It is likely important for communication between the ER and the PM, which impacts the membrane lipid composition, organization and signaling processes (Jordan et al., 2011). The importance of OSBPL8 and the polycystins has yet to be explored.

A genome-wide methylation profiling of PKD patients revealed several hypermethylated genes; among them was OSBPL8 (Woo et al., 2014). Abnormal hypermethylation leads to transcriptional silencing that can be inherited by daughter cells during cell division. PKD1 is hypermethylated in ADPKD patients, and treatment with DNA methylation inhibitors retard cyst formation. Expression changes of differentially methylated genes was found that epigenetic silencing was significant in multiple pathways

(Woo et al., 2014). The OSBP pathway could be altered in ADPKD, leading to incorrect lipid traffic, dispersion and composition; characteristics of the disease.

7.0 Future Directions

The work presented in this thesis identifies numerous PC1 and PC2 proximity interacting proteins. The screen may be repeated in triplicate to lend confidence to the identifies proximity interacting partners. The CD16.7-BirA Ciliated sample should be completed again as there were low BirA* counts in this research. Additionally, to further understand the ADPKD interactome would be to complete BioID on a PKD1 or PKD2 mutation. Currently, a graduate student in our lab has started investigating PKD1 mutations along the CTT using the same CD16.7-PKD1-BirA construct. These mutations are known point PKD-causing mutations in the final 112 aa of PC1. Understanding how the interactome changes upon mutation could provide insight on how the polycystins function, traffic and why they are important in disease mechanism and cyst formation. This data should be replicated in another kidney cell line that produces cilia such as HK-2, IMCD3, or MDCK. It will be interesting to see if and how the protein interactome changes in a different cell line.

Candidate preys, such as BLOC1S2, SYNE2, SEC63 or OSBPL8, should be investigated in respect to their relationship with ADPKD. The candidates should be examined for affect on PC1 localization to cilia using CRISPR/siRNA, as well as if they co-localize with PC1. If any candidates appear to play an important role in PC1 localization or function, their interaction should be confirmed using a secondary PPI technique such as chemical cross-linking or proximity ligation assay.

8.0 Conclusion

There remain significant gaps in our understanding of how PKD-causing genes function and traffic to primary cilia. We show that the last 112 aa of PKD1 facilitates numerous interactions that could be important in its function, traffic or interaction with PKD2. BLOC1S2, SYNE2, SEC63 and OSBPL8 were all identified as interesting candidates that could play a role in disease mechanism. This research hopes to contribute to our understanding of polycystin function and traffic, ultimately providing insight on how this disease can be treated or cured.

Appendices

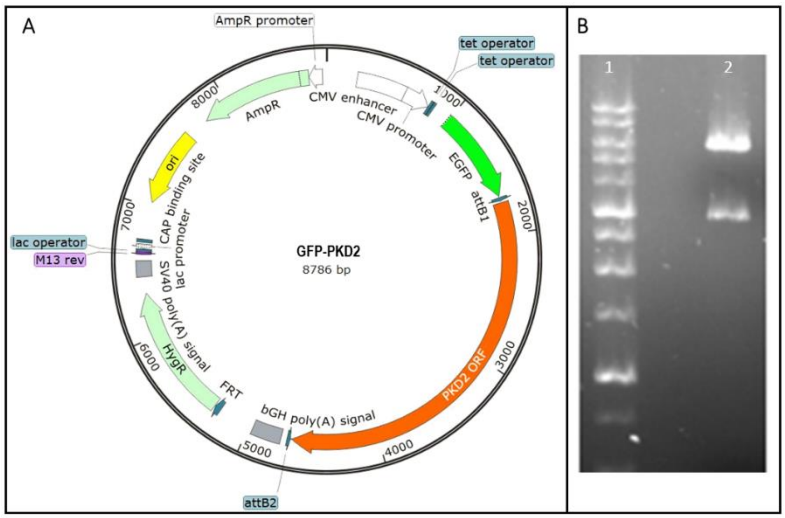

Figure S1. GFP-PKD2 Construct Cloning and Validation. ***A****: Virtual gateway cloning completed via SnapGene including PKD2 Gateway Entry clone V94950 in V4131 pDEST pcDNA5-FRT-eGFP.* ***B****: 1% agarose gel electrophoresis confirmation of V4131 pDEST pcDNA5-FRT-eGFP PKD2 Gateway Entry via restriction enzyme digest using HindIII and CutSmart NEBuffer at 50% activity, heat inactivated at 80°C for 20 minutes. Lane 1: 1 kb ladder. Lane 2. GFP-PKD2 via Gateway cloning digested.*

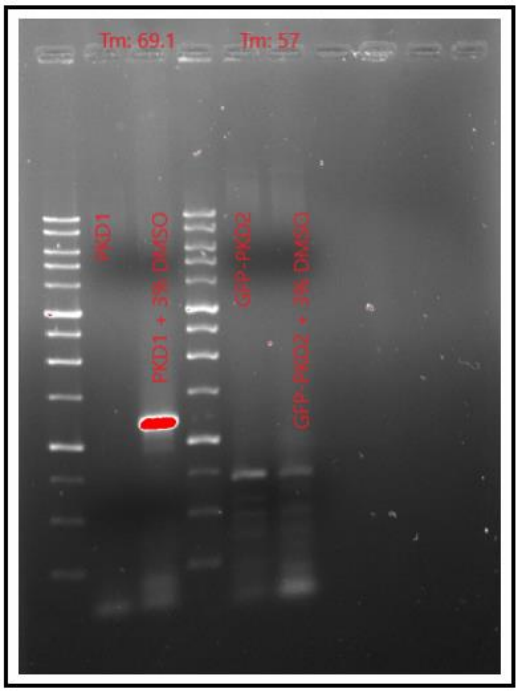

Figure S2. PCR amplification of PKD2 in attempt to clone PKD2 to have a C-terminal BirA-Flag tag. Primer melting temperature (Tm°C) for each lane is at the top. The two left most lanes are a positive control, completing the same cloning as described in figure 6. The two right-most lanes are the failed cloning attempts to amplify PKD2. Primers used were in order of forward and reverse are GACTCTAGCGTTTAAACTTAATGGTGAACTCCAGTCGCGTGC and

TATGGATCCGAGCTCGGTACGATCCCCCTACGTGGACATTAGAAC. Successful cloning was then completed by BioBasic Inc.

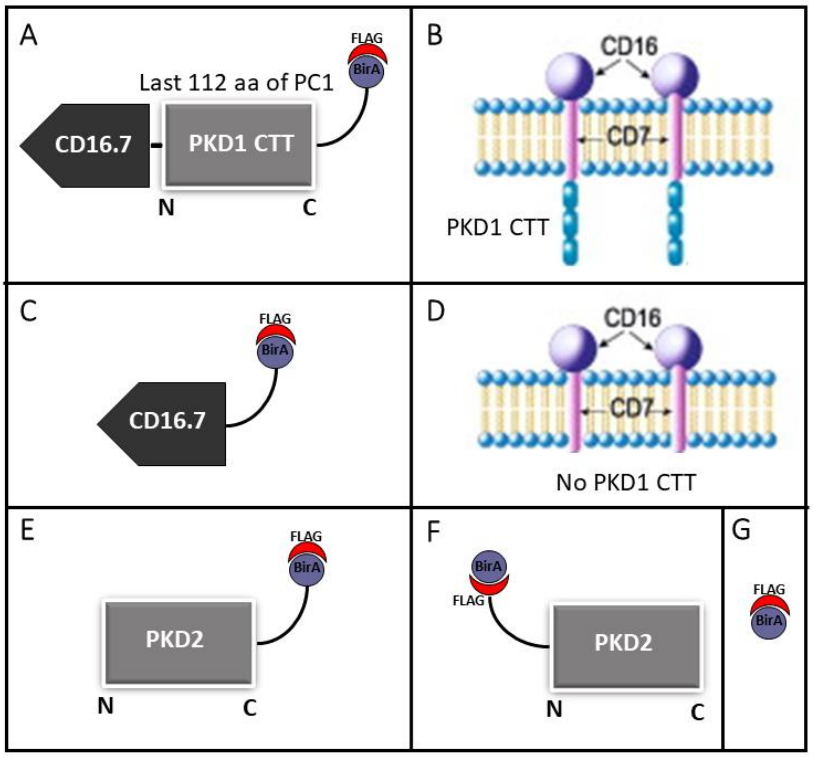

*Figure S3. Visualization of fusion constructs used for BioID. **A-B**: Fusion protein consisting of extracellular CD16 domain, transmembrane CD7 domain, the last 112 aa of PKD1 (including the binding sequence with PKD2), BirA* and a Flag-tag. **C-D**: Control for CD16.7-PKD1-BirA. This construct contains all of the same domains as A-B, except was cloned to delete the PKD1 CTT. **E**: C-terminal tagged BirA* and Flag-tag on full-length PKD2. **F**: N-terminal tagged BirA* and Flag-tag on full-length PKD2. **G**: BirA* and Flag-tag construct used as a non-specific control.*

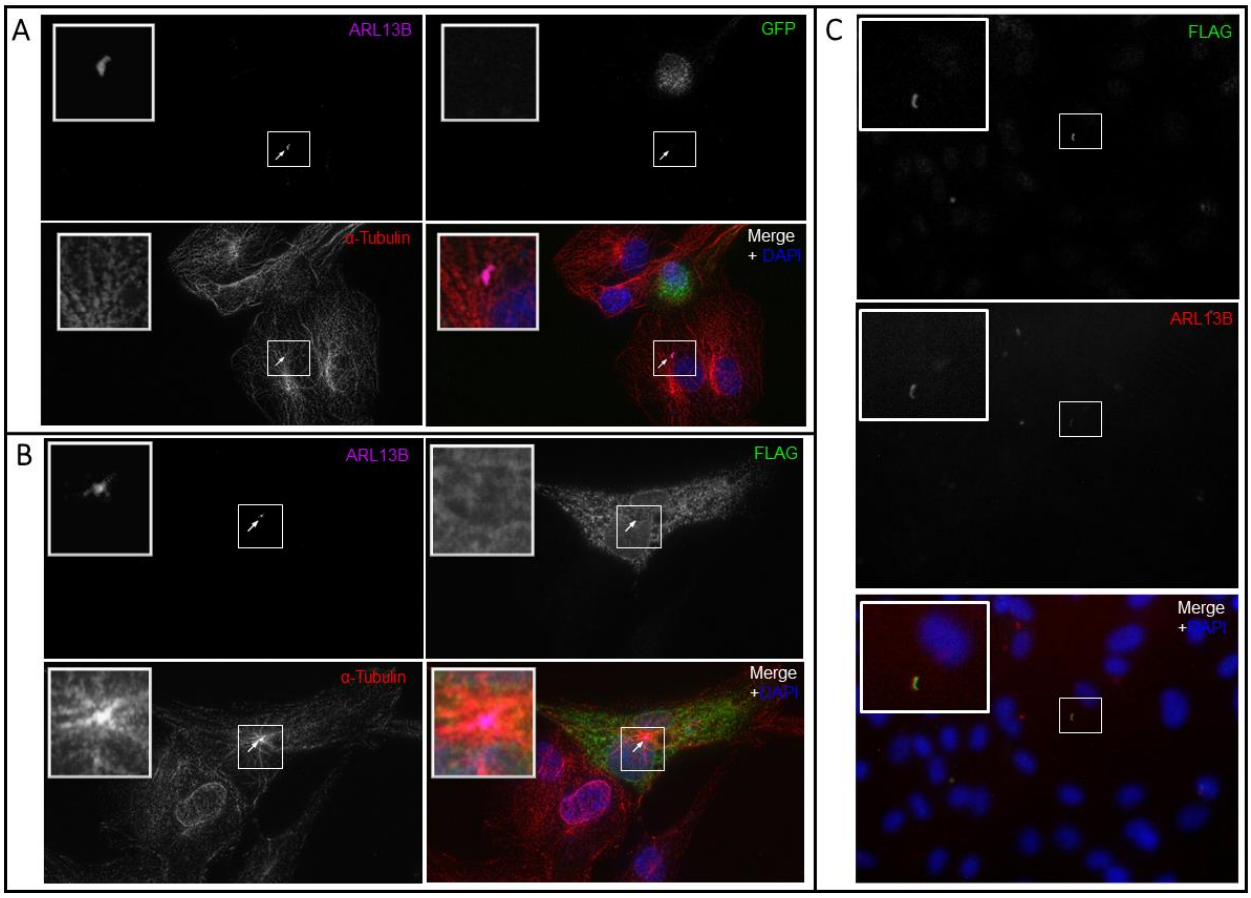

Figure S4. Localization of PC2 in hTert RPE cells. ***A****: RPE hTert cells transiently transfected with GFP-PKD2 and were subjected to immunofluorescence (IF) staining to visualize localization compared to ARL13B and α-tubulin. Localization appears to be in the ER.* ***B****: RPE hTert cells transiently transfected with BirA-PKD2 and were subjected to immunofluorescence (IF) staining to visualize localization compared to ARL13B and α-tubulin. Localization likely does not occur at cilia (ARL13B) and appears to localize in the ER.* ***C****: RPE hTert cells transiently transfected with PKD2-BirA and were subjected to immunofluorescence (IF) staining to visualize localization compared to ARL13B and α-tubulin. Localization occurs at cilia (ARL13B).*

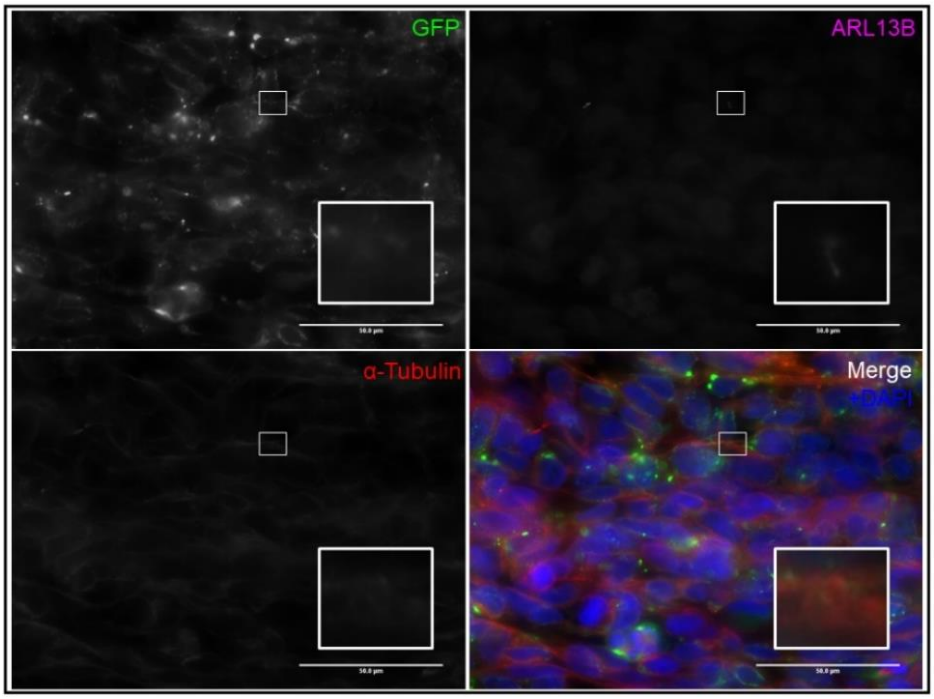

Figure S5. Stably expressing GFP-PKD2 in HEK 293 T-REx cells were subjected to IF staining to visualize cellular localization of PKD2 using anti-GFP. There is no clear evidence of co-localization with ciliary marker ARL13B using anti-ARL13B. This stable line was not used in BioID experiments.

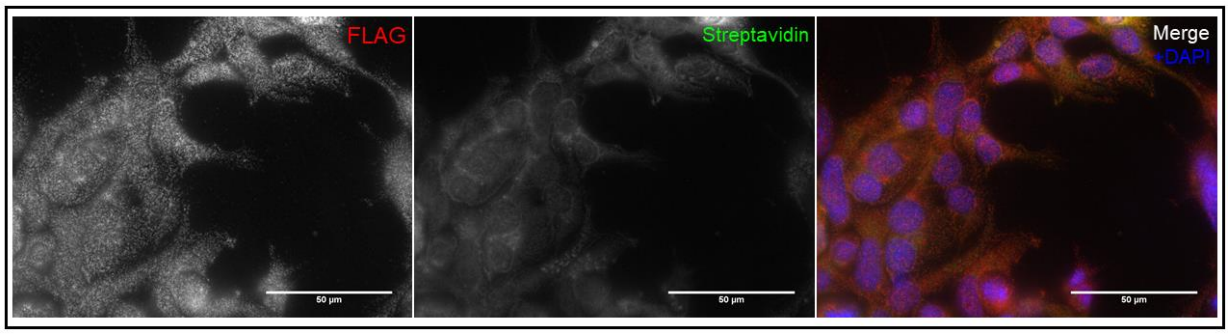

Figure S6. Stably expressing BirA-Flag in HEK 293 T-REx cells were subjected to IF staining to visualize cellular localization of BirA using anti-FLAG, and to confirm biotinylation using a Streptavidin probe (middle panel). This construct is used as a non-specific control for the BioID experiments. Localization appears to be cytosolic.

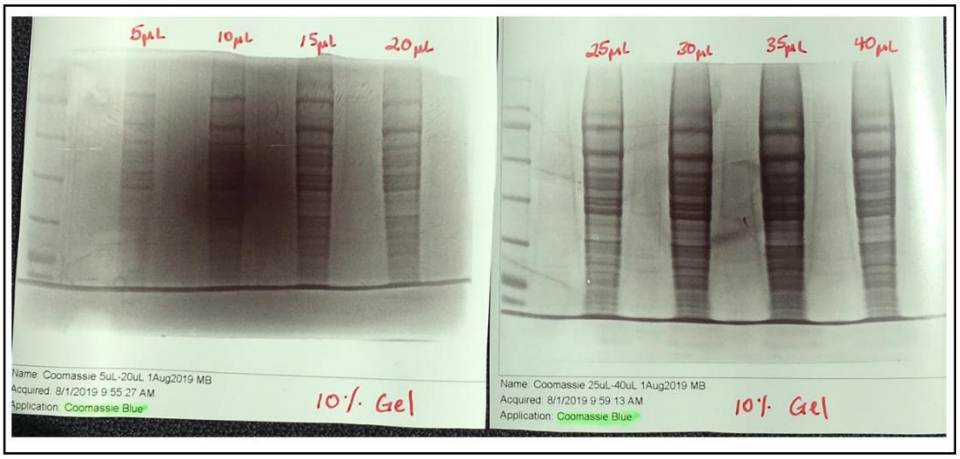

Figure S7. Coomassie Blue Stain of HEK 293 T-REx cell lysis. Each lane was lysed using MPER and 1X 1x Laemmli SDS-sample buffer, as described in the methods section. It was determined that the ideal loading volume based on the amount of protein extracted is 20μL (loading volumes are labeled at the top of each lane).

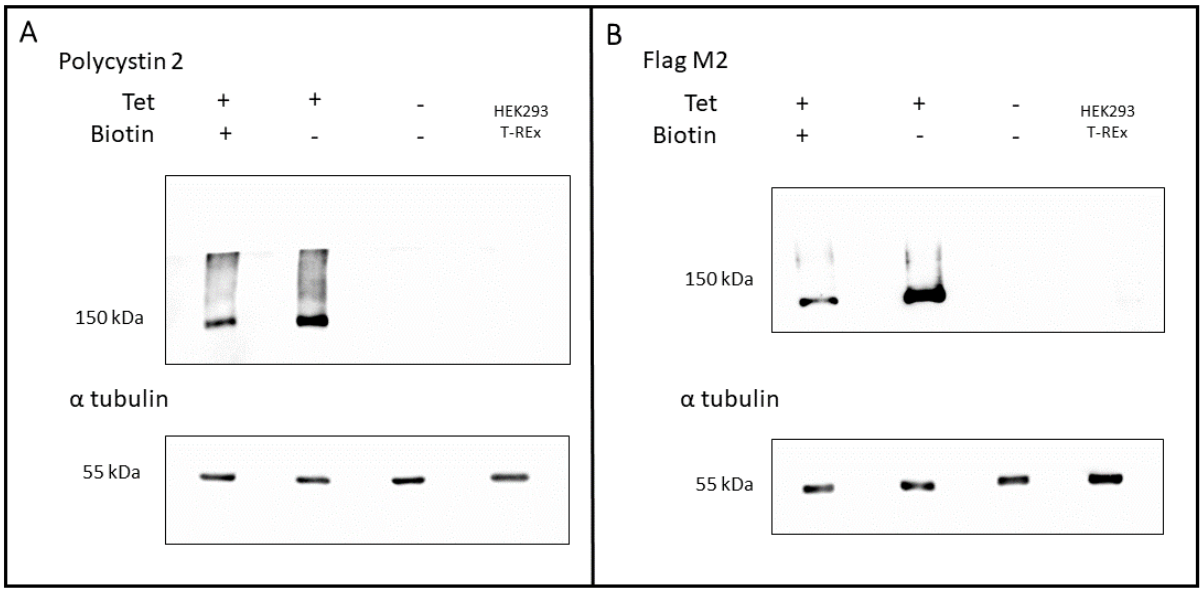

*Figure S8. Western Blot validation of BirA-PKD2 Stably Expressed in HEK 293 T-REx cells. **A**: WB validation of anti-Polycystin 2 (PC2 D3 Santa Cruz) fails to show endogenous PC2 levels in cell lysis but validates expression of BirA-PKD2 fusion protein. **B:** WB validation of BirA-PKD2 fusion protein expression using anti-FLAG.*

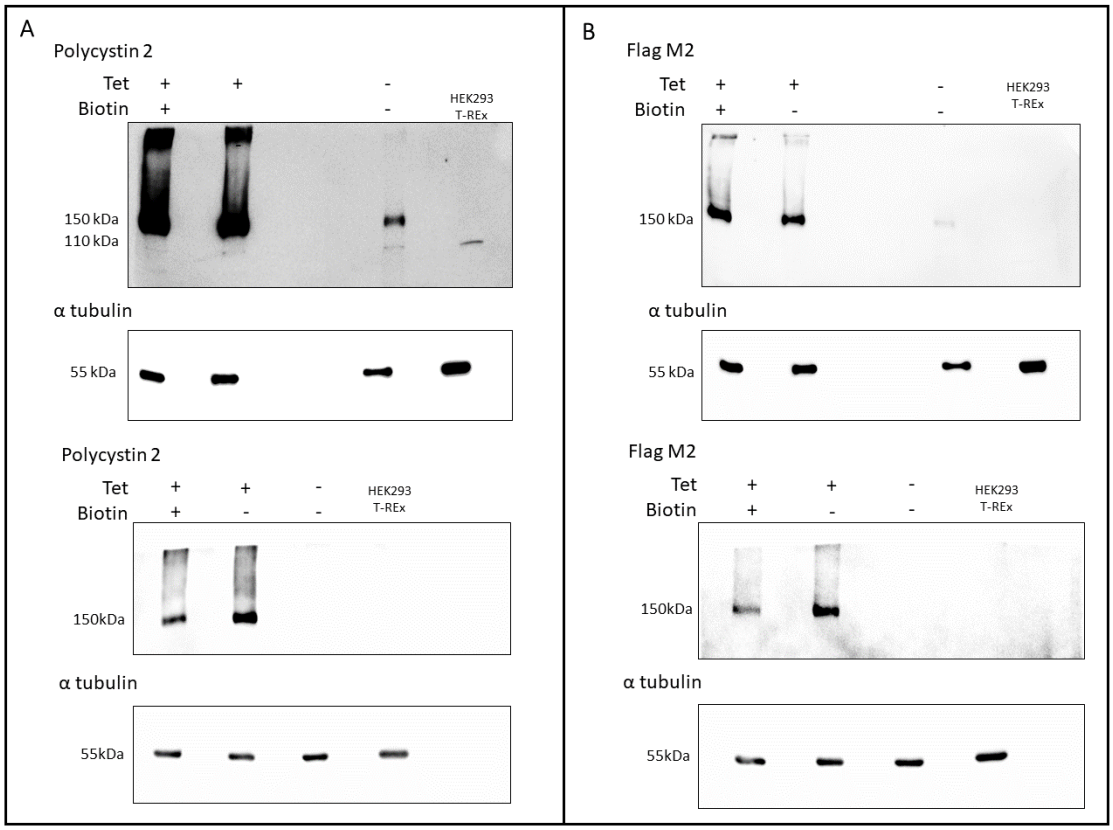

Figure S9. Western Blot validation of PKD2-BirA Stably Expressed in HEK 293 T-REx cells. ***A****: WB validation of PKD2-BirA using two different anti-Polycystin 2 antibodies. Top left, same as figure 12E (uncropped) shows endogenous PC2 levels in cell lysis and validates expression of PKD2-BirA fusion protein (PC2 YCE5 Santa Cruz). Bottom left fails to show endogenous PC2 levels in cell lysis but validates expression of BirA-PKD2 fusion protein (PC2 D3 Santa Cruz). Bands shown in Tet – samples are due to leakiness of tetracycline from FBS in the cell-culture media.* ***B****: WB validation of PKD2-BirA fusion protein expression using anti-FLAG, shown on two separate blots (top and bottom panels). The bottom panel was lysed as per the methods, but with the addition of a 1X protease inhibitor. No change in expression was detected.*

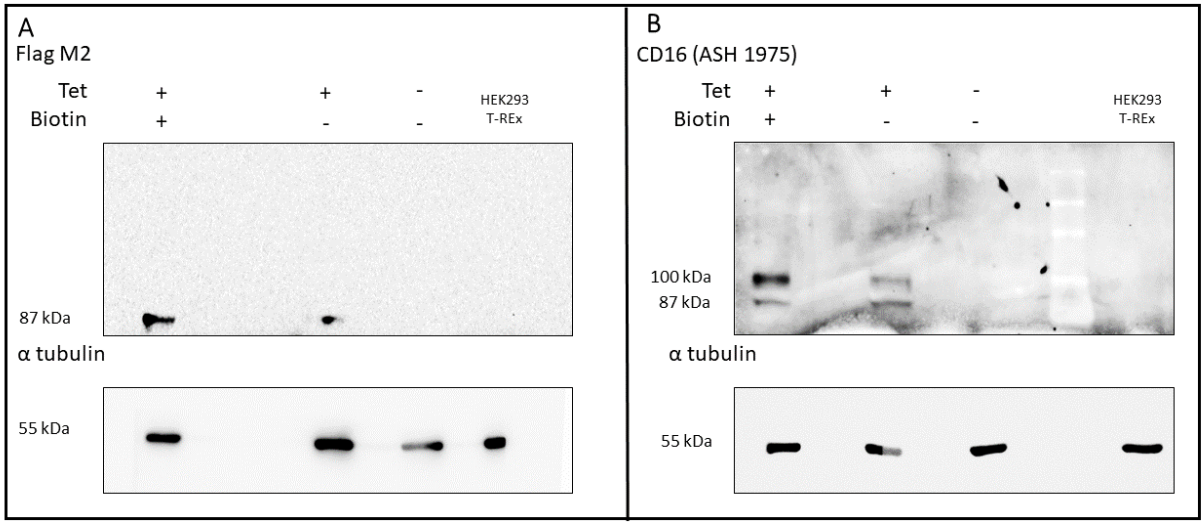

*Figure S10. Western blot validation of CD16.7-PKD1-BirA fusion protein expression using anti-FLAG (**A**) and anti-CD16 (**B**). **B**: Antibody anti-CD16 ASH 1975 (Santa Cruz) was not recommended to use on WB as per manufacturers instruction, however, successfully detected the PKD1 CTT fusion protein. Additionally, an unknown second band at 100kDa.*

Table S1. List of candidate preys from this research that overlap with various ADPKD related screens. The bait protein associated with each candidate prey can be found in the attached document "PKD1-2 BioID Data".

Gene	Impact	Reference
RASSF2	Upregulated in ADPKD patient cells	Liu et al., 2019
ANXA1	Upregulated in ADPKD patient cells	Liu et al., 2019
TUBA1A	Upregulated in ADPKD patient cells	Liu et al., 2019
SLC12A6	Downregulated in ADPKD patient cells	Liu et al., 2019
PCK2	Downregulated in ADPKD patient cells	Liu et al., 2019
SCRIB	Upregulated in tissue samples of RCAD* patients	Ricci et al., 2019
FGA	Upregulated in tissue samples of RCAD* patients	Ricci et al., 2019
PKD2	Upregulated in tissue samples of ADPKD patients	Song et al., 2009
ARL13B	Upregulated in tissue samples of ADPKD patients	Song et al., 2009
NUMBL	Upregulated in tissue samples of ADPKD patients	Song et al., 2009
CAV1	Upregulated in tissue samples of ADPKD patients	Song et al., 2009
MXRA7	Upregulated in tissue samples of ADPKD patients	Song et al., 2009
PLS1	Upregulated in tissue samples of ADPKD patients	Song et al., 2009
RAB3IP	Upregulated in tissue samples of ADPKD patients	Song et al., 2009
OSBPL8	Hypermethylated in methylation profiling of ADPKD	Woo et al., 2004
CCNB2	Upregulated in iKsp-*Pkd1*^{del} KO mice	Leonhard et al., 2019
CENPF	Upregulated in iKsp-*Pkd1*^{del} KO mice	Leonhard et al., 2019
CEP55	Upregulated in iKsp-*Pkd1*^{del} KO mice	Leonhard et al., 2019
NDC80	Upregulated in iKsp-*Pkd1*^{del} KO mice	Leonhard et al., 2019
TRIM59	Upregulated in iKsp-*Pkd1*^{del} KO mice	Leonhard et al., 2019
ZC3HAV1	Upregulated in iKsp-*Pkd1*^{del} KO mice	Leonhard et al., 2019

* RCAD: Renal Cysts and Diabetes Syndrome

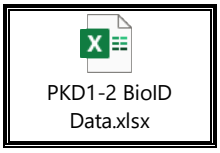

Data S1: SAINT file including all BioID baits, their associated preys, spectral count, control counts, SAINT score, fold change and BFDR.

Works Cited

Achuthan, Adrian, et al. "Regulation of the endosomal SNARE protein syntaxin 7 by colony-stimulating factor 1 in macrophages." Molecular and cellular biology 28.20 (2008): 6149-6159.

Aguilar, Andrea. "Polycystic kidney disease: SMYD2 is a novel epigenetic regulator of cyst growth." Nature Reviews Nephrology 13.9 (2017): 513.

Anyatonwu, Georgia I., and Barbara E. Ehrlich. "Calcium signaling and polycystin-2." Biochemical and biophysical research communications 322.4 (2004): 1364-1373.

Arnaiz, Olivier, et al. "Remodeling Cildb, a popular database for cilia and links for ciliopathies." Cilia 3.1 (2014): 9.

Arnould, Thierry, et al. "The polycystic kidney disease 1 gene product mediates protein kinase C α-dependent and c-Jun N-terminal kinase-dependent activation of the transcription factor AP-1." Journal of Biological Chemistry 273.11 (1998): 6013-6018.

Audrézet, M. P., Cornec-Le Gall, E., Chen, J. M., et al. (2012). Autosomal dominant polycystic kidney disease: comprehensive mutation analysis of PKD1 and PKD2 in 700 unrelated patients. Human mutation, 33(8), 1239-1250.

Bach, Horacio, et al. "Mycobacterium tuberculosis virulence is mediated by PtpA dephosphorylation of human vacuolar protein sorting 33B." Cell host & microbe 3.5 (2008): 316-322.

Badgandi, Hemant B., et al. "Tubby family proteins are adapters for ciliary trafficking of integral membrane proteins." Journal of Cell Biology 216.3 (2017): 743-760.

Barral, Duarte C., et al. "Arl13b regulates endocytic recycling traffic." Proceedings of the National Academy of Sciences 109.52 (2012): 21354-21359.

Bierings, Ruben, et al. "The interplay between the Rab27A effectors Slp4-a and MyRIP controls hormone-evoked Weibel-Palade body exocytosis." Blood, The Journal of the American Society of Hematology 120.13 (2012): 2757-2767.

Cai, Jing, et al. "A RhoA–YAP–c-Myc signaling axis promotes the development of polycystic kidney disease." Genes & development 32.11-12 (2018): 781-793.

Casuscelli, Jozefina, et al. "Analysis of the cytoplasmic interaction between polycystin-1 and polycystin-2." American Journal of Physiology-Renal Physiology 297.5 (2009): F1310-F1315.

Chapin, H. C., & Caplan, M. J. (2010). The cell biology of polycystic kidney disease. The Journal of cell biology, 191(4), 701-710.

Chebib, Fouad T., and Marie C. Hogan. "Extrarenal Manifestations of Autosomal Dominant Polycystic Kidney Disease: Polycystic Liver Disease." Polycystic Kidney Disease. Springer, New York, NY, (2018). 171-195.

Chernova, M. N., Vandorpe, D. H., Clark, J. S., & Alper, S. L. (2005). Expression of the polycystin-1 C-terminal cytoplasmic tail increases Cl-channel activity inXenopus oocytes. Kidney international, 68(2), 632-641.

Choi, Hyungwon, et al. "SAINT: probabilistic scoring of affinity purification–mass spectrometry data." Nature methods 8.1 (2011): 70.

Chung, Jeeyun, et al. "PI4P/phosphatidylserine countertransport at ORP5-and ORP8-mediated ER–plasma membrane contacts." Science 349.6246 (2015): 428-432.

Cullinane, Andrew R., et al. "Mutations in VIPAR cause an arthrogryposis, renal dysfunction and cholestasis syndrome phenotype with defects in epithelial polarization." Nature genetics 42.4 (2010): 303.

Davenport, James R., et al. "Disruption of intraflagellar transport in adult mice leads to obesity and slow-onset cystic kidney disease." Current Biology 17.18 (2007): 1586-1594.

Dulubova, Irina, et al. "How Tlg2p/syntaxin 16'snares' Vps45." The EMBO journal 21.14 (2002): 3620-3631.

Falk, Nathalie, et al. "Functional analyses of Pericentrin and Syne-2 interaction in ciliogenesis." J Cell Sci 131.16 (2018): jcs218487.

Fedeles, Sorin V., et al. "A genetic interaction network of five genes for human polycystic kidney and liver diseases defines polycystin-1 as the central determinant of cyst formation." Nature genetics 43.7 (2011): 639.

Fedeles, Sorin V., et al. "Sec63 and Xbp1 regulate IRE1α activity and polycystic disease severity." The Journal of clinical investigation 125.5 (2015): 1955-1967.

Fogelgren, Ben, et al. "The exocyst protein Sec10 interacts with Polycystin-2 and knockdown causes PKD-phenotypes." PLoS genetics 7.4 (2011).

Freedman, Benjamin S., et al. "Reduced ciliary polycystin-2 in induced pluripotent stem cells from polycystic kidney disease patients with PKD1 mutations." Journal of the American Society of Nephrology 24.10 (2013): 1571-1586.

Gainullin, Vladimir G., et al. "Polycystin-1 maturation requires polycystin-2 in a dose-dependent manner." The Journal of clinical investigation 125.2 (2015): 607-620.

Gallagher, Anna Rachel, et al. "The polycystic kidney disease protein PKD2 interacts with Hax-1, a protein associated with the actin cytoskeleton." Proceedings of the National Academy of Sciences 97.8 (2000): 4017-4022.

Ganesan, Sai J., et al. "Integrative Structure and Function of the Yeast Exocyst Complex." Protein Science (2020).

Geng, Lin, et al. "Polycystin-2 traffics to cilia independently of polycystin-1 by using an N-terminal RVxP motif." Journal of cell science 119.7 (2006): 1383-1395.

González-Perrett, S., Kim, K., Ibarra, C, et al. (2001). Polycystin-2, the protein mutated in autosomal dominant polycystic kidney disease (ADPKD), is a Ca2+-permeable nonselective cation channel. Proceedings of the National Academy of Sciences, 98(3), 1182-1187.

Harris, P. C., & Torres, V. E. (2009). Polycystic kidney disease. Annual review of medicine, 60, 321-337.

Hatsuzawa, Kiyotaka, et al. "Syntaxin 18, a SNAP receptor that functions in the endoplasmic reticulum, intermediate compartment, and cis-Golgi vesicle trafficking." Journal of Biological Chemistry 275.18 (2000): 13713-13720.

Hausman-Kedem, Moran, et al. "VPS53 gene is associated with a new phenotype of complicated hereditary spastic paraparesis." neurogenetics 20.4 (2019): 187-195.

Hodgkinson, Conrad P., Ann Mander, and Graham J. Sale. "Identification of 80K-H as a protein involved in GLUT4 vesicle trafficking." Biochemical Journal 388.3 (2005): 785-793.

Hwang, Sun-Hee, et al. "Tulp3 regulates renal cystogenesis by trafficking of cystoproteins to cilia." Current Biology 29.5 (2019): 790-802.

Ionita-Laza, Iuliana, et al. "Identification of rare causal variants in sequence-based studies: methods and applications to VPS13B, a gene involved in Cohen syndrome and autism." PLoS genetics 10.12 (2014).

Janssen, Manoe J., et al. "Loss of heterozygosity is present in SEC63 germline carriers with polycystic liver disease." PloS one 7.11 (2012).

John Peter, Arun T., et al. "The BLOC-1 complex promotes endosomal maturation by recruiting the Rab5 GTPase-activating protein Msb3." Journal of Cell Biology 201.1 (2013): 97-111.

Jonassen, Julie A., et al. "Deletion of IFT20 in the mouse kidney causes misorientation of the mitotic spindle and cystic kidney disease." The Journal of cell biology 183.3 (2008): 377-384.

Jonassen, Julie A., et al. "Disruption of IFT complex A causes cystic kidneys without mitotic spindle misorientation." Journal of the American Society of Nephrology 23.4 (2012): 641-651.

Jordan, Sabine D., et al. "Obesity-induced overexpression of miRNA-143 inhibits insulin-stimulated AKT activation and impairs glucose metabolism." Nature cell biology 13.4 (2011): 434-446.

Jung, Sung-jun, Yunjae Jung, and Hyun Kim. "Proper insertion and topogenesis of membrane proteins in the ER depend on Sec63." Biochimica et Biophysica Acta (BBA)-General Subjects 1863.9 (2019): 1371-1380.

Karniguian, Aida, Ahmed Zahraoui, and Armand Tavitian. "Identification of small GTP-binding rab proteins in human platelets: thrombin-induced phosphorylation of rab3B, rab6, and rab8 proteins." Proceedings of the National Academy of Sciences 90.16 (1993): 7647-7651.

Kathem, S. H., Mohieldin, A. M., & Nauli, S. M. (2014). The roles of primary cilia in polycystic kidney disease. AIMS molecular science, 1(1), 27.

Kim, Dae In, et al. "Probing nuclear pore complex architecture with proximity-dependent biotinylation." Proceedings of the National Academy of Sciences 111.24 (2014): E2453-E2461.

Kim, Emily, et al. "Interaction between RGS7 and polycystin." Proceedings of the National Academy of Sciences 96.11 (1999): 6371-6376.

Kim, Emily, et al. "The polycystic kidney disease 1 gene product modulates Wnt signaling." Journal of Biological Chemistry 274.8 (1999): 4947-4953.

Kim, Hyunho, et al. "Ciliary membrane proteins traffic through the Golgi via a Rabep1/GGA1/Arl3-dependent mechanism." Nature communications 5.1 (2014): 1-13.

Knudson, Alfred G. "Mutation and cancer: statistical study of retinoblastoma." Proceedings of the National Academy of Sciences 68.4 (1971): 820-823.

Korolchuk, Viktor I., et al. "Lysosomal positioning coordinates cellular nutrient responses." Nature cell biology 13.4 (2011): 453-460.

Köttgen, M. (2007). TRPP2 and autosomal dominant polycystic kidney disease. Biochimica et Biophysica Acta (BBA)-Molecular Basis of Disease, 1772(8), 836-850.

Kulikova, Sofya, et al. "Interkinetic nuclear migration: reciprocal activities of dynein and kinesin." Cell adhesion & migration 5.4 (2011): 277-279.

Kumar, Nikit, et al. "VPS13A and VPS13C are lipid transport proteins differentially localized at ER contact sites." Journal of Cell Biology 217.10 (2018): 3625-3639.

Lang, Sven, et al. "Different effects of Sec61α, Sec62 and Sec63 depletion on transport of polypeptides into the endoplasmic reticulum of mammalian cells." Journal of cell science 125.8 (2012): 1958-1969.

Langemeyer, Lars, and Christian Ungermann. "BORC and BLOC-1: Shared subunits in trafficking complexes." Developmental cell 33.2 (2015): 121-122.

Legué, Emilie, and Karel F. Liem Jr. "Tulp3 is a ciliary trafficking gene that regulates polycystic kidney disease." Current Biology 29.5 (2019): 803-812.

Lehman, Jonathan M., et al. "The Oak Ridge Polycystic Kidney mouse: modeling ciliopathies of mice and men." Developmental dynamics: an official publication of the American Association of Anatomists 237.8 (2008): 1960-1971.

Leonhard, Wouter N., et al. "Salsalate, but not metformin or canagliflozin, slows kidney cyst growth in an adult-onset mouse model of polycystic kidney disease." EBioMedicine 47 (2019): 436-445.

Li, Yuanyuan, et al. "Deletion of ADP ribosylation factor-like GTPase 13B leads to kidney cysts." Journal of the American Society of Nephrology 27.12 (2016): 3628-3638.

Liu, Dongmei, et al. "Identification of Key Genes and Candidated Pathways in Human Autosomal Dominant Polycystic Kidney Disease by Bioinformatics Analysis." Kidney and Blood Pressure Research 44.4 (2019): 533-552.

Liu, X., Vien, T., Duan, J., et al. (2018). Polycystin-2 is an essential ion channel subunit in the primary cilium of the renal collecting duct epithelium. eLife, 7, e33183.

Lo, Hsiao-Fan, et al. "Association of dysfunctional synapse defective 1 (SYDE1) with restricted fetal growth–SYDE1 regulates placental cell migration and invasion." The Journal of pathology 241.3 (2017): 324-336.

Ma, Ming, Anna-Rachel Gallagher, and Stefan Somlo. "Ciliary mechanisms of cyst formation in polycystic kidney disease." Cold Spring Harbor perspectives in biology 9.11 (2017): a028209

Magistroni, R., He, N., Wang, K., et al. (2003). Genotype-renal function correlation in type 2 autosomal dominant polycystic kidney disease. Journal of the American Society of Nephrology, 14(5), 1164-1174.

Mancias, Joseph D., and Jonathan Goldberg. "Structural basis of cargo membrane protein discrimination by the human COPII coat machinery." The EMBO journal 27.21 (2008): 2918-2928.

McNally, Kerrie E., et al. "Retriever is a multiprotein complex for retromer-independent endosomal cargo recycling." Nature cell biology 19.10 (2017): 1214-1225.

Mi, Huaiyu, et al. "PANTHER version 14: more genomes, a new PANTHER GO-slim and improvements in enrichment analysis tools." Nucleic acids research 47.D1 (2019): D419-D426.

Miller, Rachel K., ed. Kidney Development and Disease. Vol. 60. Springer, 2017.

Mochizuki, Toshio, et al. "PKD2, a gene for polycystic kidney disease that encodes an integral membrane protein." Science 272.5266 (1996): 1339-1342.

Monis, William J., Victor Faundez, and Gregory J. Pazour. "BLOC-1 is required for selective membrane protein trafficking from endosomes to primary cilia." Journal of Cell Biology 216.7 (2017): 2131-2150.

Mukhopadhyay, Saikat, et al. "TULP3 bridges the IFT-A complex and membrane phosphoinositides to promote trafficking of G protein-coupled receptors into primary cilia." Genes & development 24.19 (2010): 2180-2193.

Muppirala, Madhavi, Vijay Gupta, and Ghanshyam Swarup. "Syntaxin 17 cycles between the ER and ERGIC and is required to maintain the architecture of ERGIC and Golgi." Biology of the Cell 103.7 (2011): 333-350.

Nigro, Elisa Agnese, et al. "Polycystin-1 Regulates Actomyosin Contraction and the Cellular Response to Extracellular Stiffness." Scientific reports 9.1 (2019): 1-15.

Nozawa, Takashi, et al. "The STX6-VTI1B-VAMP3 complex facilitates xenophagy by regulating the fusion between recycling endosomes and autophagosomes." Autophagy 13.1 (2017): 57-69.

Peral, B., Ong, A. C., San Millán, J. L., et al. (1996). A stable, nonsense mutation associated with a case of infantile onset polycystic kidney disease 1 (PKD1). Human molecular genetics, 5(4), 539-542.

Perini, Enrico D., et al. "Mammalian CORVET is required for fusion and conversion of distinct early endosome subpopulations." Traffic 15.12 (2014): 1366-1389.

Perry, Ryan J., and Neale D. Ridgway. "Oxysterol-binding protein and vesicle-associated membrane protein–associated protein are required for sterol-dependent activation of the ceramide transport protein." Molecular biology of the cell 17.6 (2006): 2604-2616.

Praetorius, H. A., & Spring, K. R. (2003). The renal cell primary cilium functions as a flow sensor. Current opinion in nephrology and hypertension, 12(5), 517-520.

Pu, Jing, et al. "BORC, a multisubunit complex that regulates lysosome positioning." Developmental cell 33.2 (2015): 176-188.

Qian, F., Watnick, T. J., Onuchic, L. F., et al. (1996). The molecular basis of focal cyst formation in human autosomal dominant polycystic kidney disease type I. Cell, 87(6), 979-987.

Qian, Feng, et al. "PKD1 interacts with PKD2 through a probable coiled-coil domain." Nature genetics 16.2 (1997): 179.

Reeders, S. T., et al. "A highly polymorphic DNA marker linked to adult polycystic kidney disease on chromosome 16." Nature317.6037 (1985): 542.

Reggiori, Fulvio, et al. "Vps51 is part of the yeast Vps fifty-three tethering complex essential for retrograde traffic from the early endosome and Cvt vesicle completion." Journal of Biological Chemistry 278.7 (2003): 5009-5020.

Ricci, Pierbruno, et al. "Urinary proteome signature of Renal Cysts and Diabetes syndrome in children." Scientific reports 9.1 (2019): 1-10.

Rossetti, Sandro, et al. "Identification of gene mutations in autosomal dominant polycystic kidney disease through targeted resequencing." Journal of the American Society of Nephrology 23.5 (2012): 915-933.

Roux, Kyle J. "Dae In Kim, Manfred Raida, and Brian Burke. 2012.“A Promiscuous Biotin Ligase Fusion Protein Identifies Proximal and Interacting Proteins in Mammalian Cells.”." The Journal of Cell Biology 196.6: 801-10.

Sclip, Alessandra, et al. "Extended synaptotagmin (ESyt) triple knock-out mice are viable and fertile without obvious endoplasmic reticulum dysfunction." PloS one 11.6 (2016).

Seixas, Cecília, et al. "Arl13b and the exocyst interact synergistically in ciliogenesis." Molecular biology of the cell 27.2 (2016): 308-320.

Shayman, James A. "Targeting glucosylceramide synthesis in the treatment of rare and common renal disease." Seminars in nephrology. Vol. 38. No. 2. WB Saunders, 2018.

Smith, Elizabeth. "Autosomal Dominant Polycystic Kidney Disease–Genetics and Cyst Formation." International Journal of Clinical Pathology and Diagnosis IJCP-123. DOI 10 (2018): 2577-2139.

Solinger, Jachen A., and Anne Spang. "Tethering complexes in the endocytic pathway: CORVET and HOPS." The FEBS journal 280.12 (2013): 2743-2757.

Song, Xuewen, et al. "Systems biology of autosomal dominant polycystic kidney disease (ADPKD): computational identification of gene expression pathways and integrated regulatory networks." Human molecular genetics 18.13 (2009): 2328-2343.

Streets, A. J., Moon, D. J., Kane, M. E., Obara, T., and Ong, A. C. (2006) Identification of an N-terminal glycogen synthase kinase 3 phosphorylation site which regulates the functional localization of polycystin-2 in vivo and in vitro. Hum Mol Genet 15, 1465-1473.

Su, Qiang, et al. "Structure of the human PKD1-PKD2 complex." Science 361.6406 (2018): eaat9819.

Tang, Bor Luen, et al. "Syntaxin 12, a member of the syntaxin family localized to the endosome." Journal of Biological Chemistry 273.12 (1998): 6944-6950.

Torres, Vicente E., Peter C. Harris, and Yves Pirson. "Autosomal dominant polycystic kidney disease." The Lancet 369.9569 (2007): 1287-1301.

Tran, Pamela V., et al. "Downregulating hedgehog signaling reduces renal cystogenic potential of mouse models." Journal of the American Society of Nephrology 25.10 (2014): 2201-2212.

Tsiokas, Leonidas, et al. "Homo-and heterodimeric interactions between the gene products of PKD1 and PKD2." Proceedings of the National Academy of Sciences 94.13 (1997): 6965-6970.

Uhlen, Mathias, et al. "A pathology atlas of the human cancer transcriptome." Science 357.6352 (2017): eaan2507.

Urbina, Fabio, et al. "TRIM67 Regulates Exocytic Mode and Neuronal Morphogenesis via SNAP47." bioRxiv (2020).

Vandorpe, David H., et al. "Cation channel regulation by COOH-terminal cytoplasmic tail of polycystin-1: mutational and functional analysis." Physiological genomics 8.2 (2002): 87-98.

Vandorpe, David H., et al. "The cytoplasmic C-terminal fragment of polycystin-1 regulates a Ca2+-permeable cation channel." Journal of Biological Chemistry 276.6 (2001): 4093-4101.

Varnaitė, Renata, and Stuart A. MacNeill. "Meet the neighbors: Mapping local protein interactomes by proximity-dependent labeling with BioID." Proteomics 16.19 (2016): 2503-2518.

Veale, Kelly J., et al. "VAMP3 regulates podosome organisation in macrophages and together with Stx4/SNAP23 mediates adhesion, cell spreading and persistent migration." Experimental cell research 317.13 (2011): 1817-1829.

Venkatesh, D. (2017). Primary cilia. Journal of oral and maxillofacial pathology: JOMFP, 21(1), 8.

Wagner, Timo, et al. "Stx5 is a novel interactor of VLDL-R to affect its intracellular trafficking and processing." Experimental cell research 319.13 (2013): 1956-1972.

Walker, Rebecca V., et al. "Ciliary exclusion of Polycystin-2 promotes kidney cystogenesis in an autosomal dominant polycystic kidney disease model." Nature communications 10.1 (2019): 1-11.

Wang, Miao, et al. "SYNJ2BP promotes the degradation of PTEN through the lysosome-pathway and enhances breast tumor metastasis via PI3K/AKT/SNAI1 signaling." Oncotarget 8.52 (2017): 89692.

Wang, Shicong, et al. "A role of Rab29 in the integrity of the trans-Golgi network and retrograde trafficking of mannose-6-phosphate receptor." PloS one 9.5 (2014).

Wang, Zhaoqing, et al. "Characterization of Ceap-11 and Ceap-16, Two Novel Splicing–Variant–Proteins, Associated with Centrosome, Microtubule Aggregation and Cell Proliferation." Journal of molecular biology 343.1 (2004): 71-82.

Ward, Richard J., Elisa Alvarez-Curto, and Graeme Milligan. "Using the Flp-In™ T-Rex™ system to regulate GPCR expression." Receptor Signal Transduction Protocols. Humana Press, Totowa, NJ, 2011. 21-37.

Wartosch, Lena, et al. "Recruitment of VPS33A to HOPS by VPS16 is required for lysosome fusion with endosomes and autophagosomes." Traffic 16.7 (2015): 727-742.

Waters, A. M., & Beales, P. L. (2011). Ciliopathies: an expanding disease spectrum. Pediatric Nephrology, 26(7), 1039-1056.

Wheway, G., Nazlamova, L., & Hancock, J. T. (2018). Signaling through the primary cilium. Frontiers in Cell and Developmental Biology, 6, 8.

Wilson, P. D. (2004). Polycystic kidney disease. New England Journal of Medicine, 350(2), 151-164.

Woo, Yu Mi, et al. "Genome-wide methylation profiling of ADPKD identified epigenetically regulated genes associated with renal cyst development." Human genetics 133.3 (2014): 281-297.

Yoder, B. K. (2007). Role of primary cilia in the pathogenesis of polycystic kidney disease. Journal of the American Society of Nephrology, 18(5), 1381-1388.

Yu, Juehua, et al. "KASH protein Syne-2/Nesprin-2 and SUN proteins SUN1/2 mediate nuclear migration during mammalian retinal development." Human molecular genetics 20.6 (2011): 1061-1073.

Zeng, Jingwen, et al. "Polarized exocytosis." Cold Spring Harbor perspectives in biology 9.12 (2017): a027870.

Zhang, Xiaochang, et al. "SUN1/2 and Syne/Nesprin-1/2 complexes connect centrosome to the nucleus during neurogenesis and neuronal migration in mice." Neuron 64.2 (2009): 173-187.

Zhou, Tianhong, et al. "OSBP-related protein 8 (ORP8) regulates plasma and liver tissue lipid levels and interacts with the nucleoporin Nup62." PloS one 6.6 (2011).

Zhu, Qiuyu, et al. "Syntaxin-binding protein STXBP5 inhibits endothelial exocytosis and promotes platelet secretion." The Journal of clinical investigation 124.10 (2014): 4503-4516.

Zuo, Xiaofeng, Wei Guo, and Joshua H. Lipschutz. "The exocyst protein Sec10 is necessary for primary ciliogenesis and cystogenesis in vitro." Molecular biology of the cell 20.10 (2009): 2522-2529.